



university of
 groningen

Faculty of science and
 engineering

biomedical engineering

**Electromechanical Characterization and Modelling of
 Poly(vinylidene fluoride-trifluoroethylene-
 chlorotrifluoroethylene)-Based Soft Actuators: Films and
 Aligned Electrospun Nanofiber Mats**

Leon V. Wierenga

S3162354

Robotics Lab

Period: 06/02/2021 - 31/07/2021

Master's project

1st Examiner: [prof. dr. Raffaella Carloni - Robotics Lab]

2nd Examiner: [prof. dr. ir. GJ Verkerke - Faculty of Science and Engineering]

Table of Contents

- Article	p.3
- Abstract	p.3
- 1. Introduction	p.3
- 2. Materials	p.5
- 3. Methods	p.8
- 4. Results	p.17
- 5. Discussion	p.27
- 6. Conclusion	p.29
- Declaration of conflicting interests	p.29
- References	p.30
- Appendix	p.32
- 1. Ethics paragraph	p.32
- 2. Electrostriction Module Film Model Guide	p.34
- 3. Shell Module Film Model Guide	p.37
- 4. Shell Module Aligned Nanofiber Model Guide	p.41
- 5. Shell Module Transversely Aligned Nanofiber Model Guide	p.45
- 6. Excel data sheets	p.46

Electromechanical Characterization and Modelling of Poly(vinylidene fluoride-trifluoroethylene-chlorotrifluoroethylene)-Based Soft Actuators: Films and Aligned Electrospun Nanofiber Mats

Leon V. Wierenga (S3162354)

Abstract

Electroactive Polymers have shown to be a very good candidate for the design of a linear soft actuator with a high force-to-weight ratio and a stiffening behaviour. In this paper the electrostrictive effect of the terpolymer poly(vinylidene fluoride-trifluoroethylene-chlorotrifluoroethylene) in the form of film and aligned electrospun nanofiber mat is analyzed. In this article, the fabrication process and an experimental electromechanical characterization method is reviewed and two separate finite element analysis models are developed for analysing the bending behaviour of single layer electroactive polymers. One model will be focussing more on the electrostrictive coefficient Q-matrix in the Electrostriction Multiphysics of the commercial modelling software COMSOL Multiphysics®, while the other model will be focussing on adapting the constitutive relations for the electrostrictive materials to model the coupled behaviours explicitly in the aforementioned modelling software. The objective of this study is to validate both models to the experimental results and investigate if the models are suitable for the modelling of aligned electrospun nanofiber mats. Through quantitative comparisons, the model simulations results show good agreement with the experimental results. Furthermore, the model adapting the constitutive relations shows a good prospect for further research of aligned electrospun nanofiber integrated mats.

1. Introduction

In the first two decades of the twenty-first century, electro-active Polymers (EAPs) have become a major point of interest in various fields. Their outstanding ability to convert electrical energy into mechanical energy, by changing their shape in response to an electric stimulation, gives them a great potential to be used in many different field, such as biomedics and biorobotics as actuators or sensors in soft robotics, artificial muscles and active deployable structures [1,2]. An essential part in researching and exploring the field of EAPs, is the physics-based modelling of their electromechanical properties. Without it, the exploration of the field of EAPs would be chained to extensive, time-consuming experiments.

The EAP analyzed in this study is the relaxor ferroelectric polymer poly(vinylidene fluoride-trifluoroethylene-chlorotrifluoro-ethylene), or P(VDF-TrFE-CTFE). It has been chosen because of its large electromechanical response when exposed to an external electric field, being a high electrostrictive strain. P(VDF-TrFE-CTFE) is a terpolymer of the ferroelectric polymer polyvinylidene fluoride (PVDF). In a first step, the introduction of fluoride-trifluoroethylene (TrFE) to the polymer creates the ferroelectric copolymer poly(vinylidene fluoride-trifluoroethylene) [P(VDF-TrFE)] owning superior piezoelectric properties, high dielectric constant, low dielectric loss, and high electromechanical response, while keeping a low density. When the third bulky monomer chlorotrifluoroethylene (CTFE) is introduced, considered as structural defects into the ferroelectric copolymer P(VDF-TrFE), the

polar crystalline domain size and molecular conformation change are possibly modified. This transforms the ferroelectric copolymer into the relaxor ferroelectric terpolymer P(VDF-TrFE-CTFE). The terpolymer possesses a slim hysteresis loop, higher dielectric constant, lower Curie temperature, higher electrostriction and electromechanical response, while losing its piezoelectricity [3]. For a relaxor ferroelectric polymer like P(VDF-TrFE-CTFE) analyzed in this study, the slim hysteresis loop in combination with the possibility to orient dipoles, create the opportunity for electrostrictive strain at lower electric fields, making it an interesting EAP for soft actuation.

This study investigates whether the electromechanical and electrostrictive properties of P(VDF-TrFE-CTFE) can be modelled and therefore can be characterized mathematically. Because the overarching study is also experimentally investigating whether the actuation capabilities can be enhanced by organizing the P(VDF-TrFE-CTFE) in aligned nanofibers through electrospinning technique (mechanically stretching the nanofibers during electrospinning, enforcing an aligned configuration and therefore inducing the high density of dipoles [4]), both a homogeneous film sample and an aligned nanofiber integrated mat sample made from the P(VDF-TrFE-CTFE) material have to be modelled.

Modelling plays an important role in systematically investigating the electromechanical response and predicting the deformation and actuation forces in EAPs. For EAP-based actuation two modelling methods are commonly used: analytical modelling and Finite Element Analysis (FEA). The analytical modelling method utilizes methods like beam theory and potential energy analysis to calculate stress and deformation of a material structure, given the applied electric or magnetic field. However the structure cannot contain any complicated geometries or the method is not able to analyze the structure [5]. Therefore, in this study there is only looked into FEA models. FEA models account for all three spatial coordinates of the materials in the model and are therefore capable of predicting complex and large three-dimensional deformations of structures. Furthermore, in the physics-based FEA model, it is possible to approach a situation using different domains of physics, alter the constitutive equations to add a multi-domain relation and easily in specific cases combine different physics domains to create a multiphysics domain.

For example, Poncet et al. (2017) used analytical calculations alongside a developed FEA model to describe the piezoelectric behavior of a P(VDF-TrFE) cantilever actuator by modelling their test setup in the commercially available modelling programme COMSOL Multiphysics®.[6] By combining the Structural Mechanics and Electrostatics Module into the Multiphysics Electromechanical Forces and Piezoelectric Effect in the program, the electromechanical response of the PVDF-based EAP P(VDF-TrFE) could be modelled. In this study, the analytical calculations verified the FEA model.

A study done by Zhang et al. (2020) on the electromechanical coupling in electroactive polyurethane chose a similar approach. In this study, the electromechanical response of the EAP polyurethane is modelled in the COMSOL Multiphysics® software, using the Electromechanical Forces Multiphysics, connecting the electric domain and solid mechanics domain. The polyurethane used in this study, rather than being expressing a piezoelectric behaviour, shows electrostrictive behaviour combined with the Maxwell stress. This electromechanical response could be recreated in the FEA model and they were therefore able to characterize the EAP electromechanical coupling behaviour.[7]

On the other hand, FEA models approximating the effect of an applied electric field by applying a pair of compressive surface tractions of equal magnitude but in opposite directions to study actuation performance of a dielectric elastomer and PVDF-based terpolymer have also been developed by for example McGough et al. (2014) [8]. However, a major limitation of this approach is that net forces will occur especially at high deformations because of imbalance of surface areas on two sides. This will lead to significant deviation from experimental results, especially for thin structures.

Lastly, Zhang et al. (2018) applied a new method, shell theory, to approximate a P(VDF-TrFE-CTFE) thin film actuator and a magnetoactive elastomer (MAE) [5]. By altering the constitutive equations for mechanical strain within the modelling program, they were able to add the strain generated by the electric field via electromechanical coupling to the model and calculate the displacement of the EAP thin film in 3 spatial dimensions. This modelling method avoids the use of equivalent surface traction (i.e. Maxwell stress) and instead models direct electromechanical and magneto-mechanical couplings explicitly in the constitutive equations, in order to better predict the responses of the EAP when an external electric or magnetic field is applied. Although the model was simplified (considering the materials to be isotropic, considering the electric field to be always applied through the thickness of the material and not taking into account any residual stresses at rest) to decrease the amount of nodes in the model, it showed to be very accurate to experimental data. This way of modelling was also reused in later studies of Zhang et al. and was also adopted by different researchers for the modelling of a similar experiment.[9]

This study will be a first attempt at modelling the electromechanical response of an electroactive polymer thin film using two different modelling methods to an experimental test-setup. The modelling methods will be based on results obtained from an experimental setup measuring the electromechanical response of the P(VDF-TrFE-CTFE) film and nanofiber samples. In the remainder of this article, the experimental test setup and the gathering of the data will be explained, next the constitutive equations of the terpolymer-based actuations will be introduced, and their implementation into the FEA model will be explained. Then, the FEA models are developed using the modelling programme COMSOL Multiphysics® software. There will be made use of the modelling method using the shell theory, proposed in the paper by Zhang et al. (2018) and a model will be made with the use of a new module introduced in COMSOL Multiphysics® version 5.6 (<https://www.comsol.com/release/5.6>). This version of COMSOL introduces Ferroelectric Material Models in the Electrostatics Module and introduces a new Electrostriction Multiphysics module. Two models are created to analyze the possibility to predict the behaviour of electroactive polymer based actuators with either a model that includes a multiphysics coupling to predict the actuators behaviour or a model where the electromechanical constitutive equations are explicitly inserted. Subsequently, it will be investigated if one or both of the models can be modified to become suitable for modelling an EAP-nanofiber integrated mat.

2. Materials

The polymeric material, Solvne T® P(VDF-TrFE-CTFE), analyzed in this study is provided by Solvay Specialty Polymers (Solvay S.p.A., Milano, Italy, www.solvay.com). The Solvne T® P(VDF-TrFE-CTFE) contains 63 mol% VDF, 28 mol% TrFE and 9 mol% CTFE (63/28/9 mol%).

the dielectric constant $\epsilon_r = 45$ at 1kHz and a Curie temperature of 16°C. The introduction of the chlorotrifluoroethylene (CTFE) monomer as a defect into the ferroelectric P(VDF-TrFE) copolymer causes the terpolymer to lose its piezoelectric properties, leaving its electromechanical response to be only its high electrostrictive strain, producing a large field-induced strain, when exposed to an external electric field.[10]

P(VDF-TrFE-CTFE) films

With regards to studies previously done by the research group, the fabrication of the films of P(VDF-TrFE-CTFE) has stayed unchanged.[4] The films have been realized by melt extrusion and have been cut to obtain specimens. The dimensions are shown in table 1.

Material	Length (l) [mm]	Width (b) [mm]	Thickness [mm]
P(VDF-TrFE-CTFE) film "sample 5"	65	11	0.135
P(VDF-TrFE-CTFE) film "sample 6"	65	11	0.150
PVDF-TrFE-CTFE) nanofiber integrated PDMS mat	65	11	0.100
Kapton H® Tape	65	11	0.057

Table 1. Spatial dimensions (length, Width, Thickness) of the specimens of P(VDF-TrFE-CTFE) film ("sample 5" and "sample 6") and P(VDF-TrFE-CTFE) electrospun nanofiber integrated PDMS mats and passive material.

P(VDF-TrFE-CTFE) Electrospun Nanofiber mats

The fabrication process of the P(VDF-TrFE-CTFE) aligned nanofibers has also stayed unchanged since the previously done study by the research group. The nanofibers were fabricated by electrospinning technique. A solution of P(VDF-TrFE-CTFE) powder (30 wt%) and Acetone:DMF 55:45 (w/w) was processed by an electrospinning machine (Spinbow™, Bologna, Italy, www.spinbow.it/en). The machine is equipped with four needles with a length of 55 mm and an internal diameter of 0.84 mm. The needles are connected to 5 mL syringes via PTFE tubings. The nanofibers are collected on a poly(ethylene)-coated paper covered rotating drum. The settings of the electrospinning machine are summarized in table 2.

Flow rate	0.8 [mL/h]
Electric potential	26 [kV]
Drum rotation speed	2430 [rpm]
Distance needles-drum	14 [cm]
Relative humidity	52 [%]

Temperature	20 [°C]
-------------	---------

Table 2. Setting used in the electrospinning machine for the production of the P(VDF-TrFE-CTFE) nanofiber mats.

The P(VDF-TrFE-CTFE) electrospun nanofibers have been integrated into a silicone matrix (PDMS) through a blading process and cured to obtain specimens. The spatial dimensions of the P(VDF-TrFE-CTFE) electrospun nanofiber integrated PDMS mat are shown in table 1.

Other materials: Passive Layer and Electrodes

For the passive layer, the material Kapton H® is used, as it is commonly used in flexible electronics, because of its stability in a wide range of temperatures. For the electrodes, a layer of gold is sputtered onto the P(VDF-TrFE-CTFE). For the electrospun nanofibers of P(VDF-TrFE-CTFE) integrated in PDMS, silicon based electrodes doped with 17.5% of carbon black are realized. This is due to experimental difficulties on the deposition of gold nanoparticles on the PDMS surface.

Structure of the actuators

The final design of the P(VDF-TrFE-CTFE) film consists of an active layer of homogeneous P(VDF-TrFE-CTFE) film, sputtered on both the top and bottom sides with a layer of gold, serving as electrodes. A layer of Kapton H® serves as a passive layer. The P(VDF-TrFE-CTFE) nanofiber sample consists of an active layer of electrospun nanofibers integrated in a PDMS matrix. On both sides of the mat, silicon-based electrodes are present. On the top side of the active layer a layer of Kapton H® serves as a passive layer. (figure 1.)

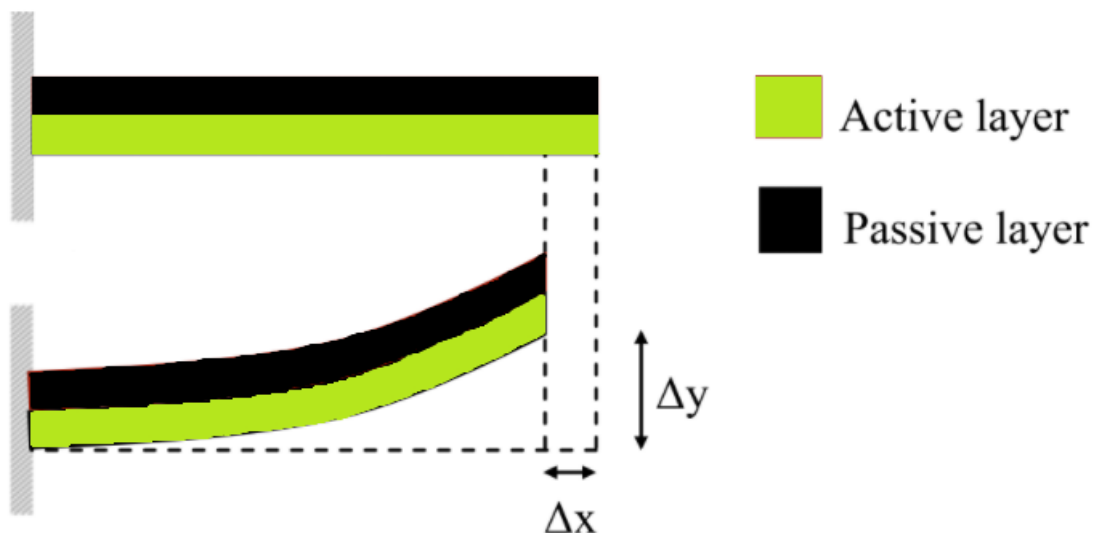


Figure 1. Schematic representation of the fabricated actuator. Top: unloaded actuator, bottom: actuator exposed to an electric field.

When an external electric field is applied across the P(VDF-TrFE-CTFE), a strain is produced in its longitudinal axis due to the synergistic effect of the Maxwell stress (i.e., the electrodes are attracted to each other and, as a consequence, the P(VDF-TrFE-CTFE) is mechanically compressed in the thickness direction and expands in the longitudinal directions) and the

electrostriction (i.e., the applied electric field induces a conformational change of polymer chain that may produce a large strain in thickness). The passive layer, with its different elastic modulus, resists the deformation, resulting in the bending of the P(VDF-TrFE-CTFE)-based actuators.

3. Methods

In this study, a combination of data obtained from literature and experimentally gathered data is used to provide enough information about the P(VDF-TrFE-CTFE) samples on their mechanical and electromechanical material properties and their electromechanical response in order for a physics-based model of the experiment to be created. This means the study is structured like a triptych: Data Collection, Mathematical Formulation and COMSOL Implementation.

Data collection

The data collecting on both the P(VDF-TrFE-CTFE) film and P(VDF-TrFE-CTFE) nanofiber integrated PDMS mat consists of 2 parts: Mechanical Characterization of the Active Material and Experimentally Measuring the Electromechanical Response. The gathering of the data for both parts is done via the methods used in a previous study of our research team.

Mechanical Characterization

Transverse Isotropic Nanofibers

While the homogeneous P(VDF-TrFE-CTFE) film can be seen as an isotropic material, the electrospun P(VDF-TrFE-CTFE) nanofibers cannot, since the material properties are no longer unidirectional. Nanofibers materials can instead be seen as transverse isotropic materials: orthotropic materials with physical properties that are symmetric about an axis that is normal to a plane of isotropy. This means that the P(VDF-TrFE-CTFE) nanofibers have distinct axial and transversal mechanical properties, with the transversal properties being isotropic. For modelling purposes, this makes the modelling of the nanofibers easier, since the number of variables in the mechanical properties is only 5: the Young's Modulus in axial direction, Young's Modulus in transverse direction, the Poisson's ratio between the axial and transverse direction, Poisson's ratio between the transverse directions and the Shear Modulus in the transverse plane, respectively $E_a, E_t, \nu_{12}, \nu_{23}, G_{23}$.

Young's Modulus

The Young's Moduli of the different specimens of both the P(VDF-TrFE-CTFE) film and P(VDF-TrFE-CTFE) nanofibers and the passive layers have been evaluated in tensile tests with the ElectroPuls E1000 (Instron™, Norwood (MA),USA,www.instron.us). For the passive layers, it is equipped with either a 2kN Instron™ static load cell 2527-129, for the electro-active P(VDF-TrFE-CTFE) film or P(VDF-TrFE-CTFE) nanofiber integrated PDMS mat layer with a5N Instron™ static load cell 2530-5N. The tensile tests for each material have been repeated three times. For each material, the average of these three tests was noted as a parameter to be used in the model.

The Young's Moduli of the P(VDF-TrFE-CTFE) nanofiber composite sample could be approximated by using the mixture theory, adding up the fractional Young's Moduli of the isotropic PDMS matrix and the transverse isotropic P(VDF-TrFE-CTFE) nanofibers.

Not all directional Young's Moduli of each P(VDF-TrFE-CTFE) nanofiber composite sample could be evaluated in the tensile tests. The Young's Modulus of the fibers through the thickness, in z-direction, could not experimentally be determined with the equipment available in our laboratory. Therefore, by following the transverse isotropic material property theory, the Young's Modulus in the direction of the thickness was set to be the same as in the other transversal direction.

Dielectric Permittivity

The P(VDF-TrFE-CTFE) film samples have been realized by melt extrusion. They possess a dielectric constant $\epsilon_r = 45$ at 1kHz. The dielectric constant of the P(VDF-TrFE-CTFE) nanofiber layer has been evaluated with the Alpha dielectric analyzer (Novocontrol Technologies GmbH & Co.KG, Montabaur, Germany, www.novocontrol.de).

Poisson's ratio

The Poisson's ratio of the isotropic P(VDF-TrFE-CTFE) film in literature was found to be approximately in between 0.22 to 0.33, depending on the mol% of CTFE in the material.[12, 13] This percentage changes the mechanical properties of the polymer, making the terpolymer more or less squeezable by the attraction between the electrodes. The Solvane T® P(VDF-TrFE-CTFE) used in this study has a 63 mol% VDF, 28 mol% TrFE and 9 mol% CTFE (63/28/9 mol%) ratio. Following the values shown in [12], the Poisson's ratio assigned to the P(VDF-TrFE-CTFE) film is 0.22.

The Poisson's ratios of the transverse isotropic P(VDF-TrFE-CTFE) nanofiber mats are intuitively different to the Poisson's ratio of the isotropic P(VDF-TrFE-CTFE) film and could also not be found in literature. Since it is not convenient to measure the transverse strains directly to calculate the Poisson's ratios from them, due to the compliance of the terpolymer layer, the Poisson's ratios between the axial and transversal directions were instead approximated by using a different method: the poisson's ratio for orthotropic materials can be approximated by using the directional Young's Moduli of the orthotropic material (equation (1)). [14]

$$|v_{12}| < (E_2/E_1)^{1/2} \quad (1)$$

Since the Young's Moduli in axial and transversal direction are experimentally obtained, the Poisson's ratio between axial and transversal strain of the nanofibers can be approximated. This method is used in a first approximation. In a later design, a method to experimentally evaluate the Poisson's ratios could be used. The Poisson's ratio in the transverse plane was estimated by using literature on the relation between the transverse strains in other transverse isotropic materials.[15] These transverse Poisson's ratios are extremely low [0.01 - 0.06]. For the P(VDF-TrFE-CTFE) nanofibers, a Poisson's ratio in this range was chosen. Using the mixture theory, the final Poisson's ratio between axial and transversal strain of the complete composite material was determined.

Mixture Method for Composite materials

While the P(VDF-TrFE-CTFE) film can be approached as a homogeneous isotropic material, the P(VDF-TrFE-CTFE) nanofiber integrated PDMS samples are classified as a fibrous composite material. In order to be able to obtain the mechanical properties of the composite material, the Mixture Method has been applied to approximate the final mechanical properties of the composite [11]. First the volumetric fractions of the P(VDF-TrFE-CTFE) nanofibers and the PDMS matrix were determined. Subsequently, for every mechanical property of every component in the composite material, the obtained value was multiplied by the volumetric fraction of that component and the two fractional properties were added to create the final mechanical property value (equation (2) for Young's Modulus in x-direction).

$$X_{composite} = X_{nanofiber} * V_f + X_{matrix} * V_m \quad (2)$$

With the net mechanical property of the composite $X_{composite}$, the mechanical property of the nanofibers $X_{nanofiber}$, the volumetric fraction of the fibers V_f , the mechanical property of the matrix X_{matrix} , and the volumetric fraction of the matrix V_m .

Experimentally Recording of the Electromechanical Response

To experimentally determine the electromechanical response of the P(VDF-TrFE-CTFE) film and nanofiber integrated mat, in an experimental setup the tip displacement of the samples is recorded under electric fields of different strengths.

A digital m7915mztl 5 MPx microscope (Dino-Lite, AnMo Electronics Corp, Taipei, Taiwan, www.dino-lite.com) is used to record the displacement of the actuator's tip under different electric field strengths. The displacement is recorded in a video with the DinoCapture software (version 2.0) which is, then, analyzed in Matlab (Mathworks, USA) with a computer vision script. The overall experimental test setup for measuring the tip displacement is shown in figure 2.

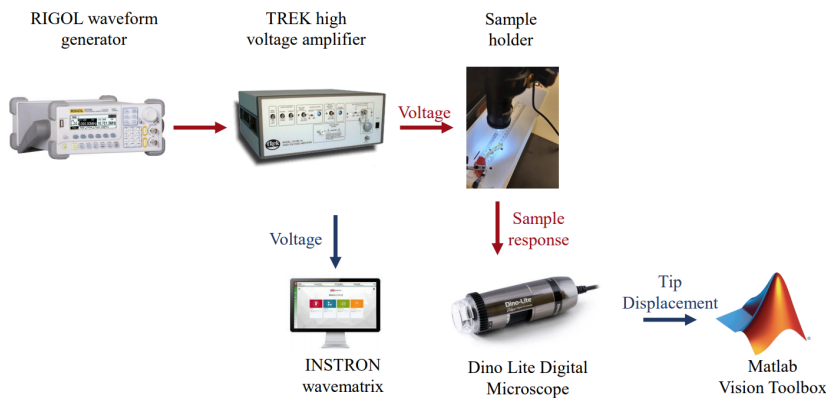


Figure 2. Experimental test setup for measuring the tip displacement of the P(VDF-TrFE-CTFE) film and nanofiber mat actuators: The TREK 10/10B-HS high-voltage amplifier, operated through the RIGOL DG1022 waveform generator, applies a voltage to the actuator. The tip displacement is captured with the digital m7915mztl 5 MPx microscope and processed in MATLAB.

Mathematical Formulation

Electrostriction Module

When using the Electrostriction and Electromechanical Forces Module, the electrostrictive response of the P(VDF-TrFE-CTFE) material can be modelled as a quadratic coupling of the electrostrictive strain tensor ε_{ij} to the electric polarization density P_m using the electrostrictive coefficient Q_{ijkl} . The contribution of the Maxwell stress model can be differentiated into the elastic strain ε_s from a spring and the viscous strain ε_d from a dashpot. The elastic strain is dependent on the applied stress σ and the Young's Modulus E . The viscous strain is determined by the relation between the applied stress σ on the dashpot and the dashpot constant η [16]. The complete relation is shown in equation (3).

$$\begin{aligned}\varepsilon_t &= \varepsilon_{el} + \varepsilon_s + \varepsilon_d \\ \varepsilon_{ij} &= Q_{ijkl} P_k P_l + \frac{\sigma}{E} + \frac{\sigma}{\eta}\end{aligned}\quad (3)$$

For the isotropic film sample, Q11 is found in literature to be equal to $-12 M^4/C^2$. [17] Since Q12 depends on the spatial dimensions of the sample, this value will be different for different sizes of film samples. Because Q12 is the only remaining unknown parameter, it is decided to run the model for different values of Q12 to find the value for which the simulation is best fitting the experimental data.

For the transverse isotropic P(VDF-TrFE-CTFE) nanofibers mat, the complete electrostrictive Q-matrix of the P(VDF-TrFE-CTFE) material is required as an input. This data is not available in literature and would only be able to be obtained from experiments. Unfortunately, it has not been able to perform such experiments due to insufficient lab instruments and equipment. It is also not viable to run the model for different values of this Q-matrix, since instead of 1 unknown parameter there is now an unknown 6-by-6 matrix.

Shell Module

When using the Shell Module, the electrostrictive response of the P(VDF-TrFE-CTFE) material can be modelled as a quadratic coupling between strain and the electric field, adding an additional electromechanical element to the stress-strain relation. The expression of strain ε_{ij} can then be written in terms of stress σ_{kl} and electric field E_k, E_l as is shown in equation (4). [18, 19]

$$\varepsilon_{ij} = S_{ijkl} \sigma_{kl} + M_{ijkl} E_k E_l \quad (4)$$

Here S_{ijkl} is the elastic compliance tensor and M_{ijkl} represents the electromechanical coupling coefficient tensor, that comprises the Maxwell stress effect and the electrostrictive response. As done in the article by Zhang et al. (2018) [5], several simplifications and assumptions are made based on experimental conditions and material symmetries. For the film sample, all materials are assumed to be mechanically isotropic. For the nanofiber sample, the

nanofiber specimen is considered to be mechanically transverse isotropic, while the other materials are assumed to be mechanically isotropic. The electric field is always applied through the thickness direction of the active layer, therefore the only non-zero term in the electric field vector is E_3 . There is considered to be no residual stress when the materials are at rest. Lastly, the tensors are converted into reduced-symmetry matrices using Voigt notation. Thus the constitutive relation between strain and the electric field, taking all assumptions and simplifications into account is shown in equation (5).

$$\epsilon_i = S_{ij} \sigma_j + M_{ij} E_j^2 \quad (5)$$

Because the FEA modelling programme expresses Hooke's law in stiffness form, where stress is written in terms of strain, the added quadratic coupling effects of the electric field changes that equation to equation (6).

$$\sigma_j = S_{ij}^{-1} (\epsilon_i - M_{ij} E_j^2) \quad (6)$$

For the mechanically isotropic film, equation (6) can be expanded to equation (7):

$$\begin{pmatrix} \sigma_1 \\ \sigma_2 \\ \sigma_3 \\ \sigma_4 \\ \sigma_5 \\ \sigma_6 \end{pmatrix} = \begin{bmatrix} \lambda + 2\mu & \lambda & \lambda & 0 & 0 & 0 \\ \lambda & \lambda + 2\mu & \lambda & 0 & 0 & 0 \\ \lambda & \lambda & \lambda + 2\mu & 0 & 0 & 0 \\ 0 & 0 & 0 & 2\mu & 0 & 0 \\ 0 & 0 & 0 & 0 & 2\mu & 0 \\ 0 & 0 & 0 & 0 & 0 & 2\mu \end{bmatrix} \begin{pmatrix} \epsilon_1 \\ \epsilon_2 \\ \epsilon_3 \\ \epsilon_4 \\ \epsilon_5 \\ \epsilon_6 \end{pmatrix} - \begin{bmatrix} M_{11} & M_{12} & M_{13} & 0 & 0 & 0 \\ M_{21} & M_{22} & M_{23} & 0 & 0 & 0 \\ M_{31} & M_{32} & M_{33} & 0 & 0 & 0 \\ 0 & 0 & 0 & M_{44} & 0 & 0 \\ 0 & 0 & 0 & 0 & M_{55} & 0 \\ 0 & 0 & 0 & 0 & 0 & M_{66} \end{bmatrix} \begin{pmatrix} 0 \\ 0 \\ E_3^2 \\ 0 \\ 0 \\ 0 \end{pmatrix} \quad (7)$$

Where the two Lamé constants λ and μ are expressed as:

$$\lambda = \frac{Ev}{(1+v)(1-2v)}$$

$$\mu = \frac{E}{2(1+v)}$$

With E and ν being the Young's Modulus and Poisson's ratio of the terpolymer respectively.

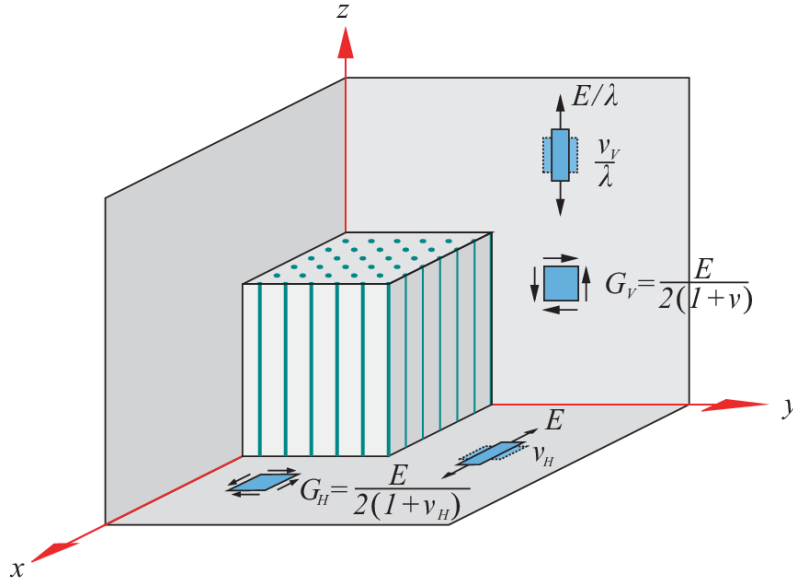


Figure 3. Transversely isotropic medium with visualization of the symmetry and definition of elastic constants.[20]

For the mechanically transverse isotropic nanofibers, visualized in figure 3, the relation between the mechanical properties in the axis of symmetry and on the symmetry plane is different as shown in the figure. For transverse isotropic materials equation (6) can be expanded to equation (8).[20]

$$\begin{bmatrix} \sigma_1 \\ \sigma_2 \\ \sigma_3 \\ \sigma_4 \\ \sigma_5 \\ \sigma_6 \end{bmatrix} = \begin{bmatrix} C_{11} & C_{12} & C_{13} & 0 & 0 & 0 \\ C_{12} & C_{11} & C_{13} & 0 & 0 & 0 \\ C_{13} & C_{13} & C_{33} & 0 & 0 & 0 \\ 0 & 0 & 0 & C_{44} & 0 & 0 \\ 0 & 0 & 0 & 0 & C_{44} & 0 \\ 0 & 0 & 0 & 0 & 0 & \frac{1}{2}(C_{11} - C_{12}) \end{bmatrix}$$

$$\begin{pmatrix} \begin{bmatrix} \varepsilon_{xx} \\ \varepsilon_{yy} \\ \varepsilon_{zz} \\ 2\varepsilon_{xz} \\ 2\varepsilon_{yz} \\ 2\varepsilon_{xy} \end{bmatrix} - \begin{bmatrix} M_{11} & M_{12} & M_{13} & 0 & 0 & 0 \\ M_{21} & M_{22} & M_{23} & 0 & 0 & 0 \\ M_{31} & M_{32} & M_{33} & 0 & 0 & 0 \\ 0 & 0 & 0 & M_{44} & 0 & 0 \\ 0 & 0 & 0 & 0 & M_{55} & 0 \\ 0 & 0 & 0 & 0 & 0 & M_{66} \end{bmatrix} \begin{bmatrix} 0 \\ 0 \\ E_3^2 \\ 0 \\ 0 \\ 0 \end{bmatrix} \end{pmatrix} \quad (8)$$

Where

$$\begin{aligned}
C_{11} &= \frac{E(\lambda - v_v^2)}{(\lambda - \lambda v_H - 2v_v^2)(1 + v_H)} & C_{33} &= \frac{(1 - v_H)E}{(\lambda - \lambda v_H - 2v_v^2)} \\
C_{12} &= \frac{E(\lambda v_H + v_v^2)}{(\lambda - \lambda)} & C_{44} &= \frac{E}{2(1 + v)} \\
C_{13} &= \frac{v_v E}{(\lambda - \lambda v_H - 2v_v^2)} & \frac{1}{2}(C_{11} - C_{12}) &= \frac{E}{2(1 + v_H)}
\end{aligned}$$

Using the Young's Modulus in the transverse directions E , the Poisson's ratio in the plane perpendicular to the axis of symmetry v_H , the Poisson's ratio along the symmetry axis v_v and the ratio between the Young's Modulus in the transverse directions and the Young's Modulus in the axial direction $\lambda = E_{transverse}/E_{axial}$. The electromechanical term for this

Since E_3 is the only non-zero term in the electric field vector, M_{13} , M_{23} and M_{33} are the only effective electrostrictive coefficients in both linear elastic material models that will have an impact on the electromechanical response of the terpolymer. As mentioned for the determination of the Poisson's ratios of the nanofiber samples, it is not convenient to measure the transverse strains directly. Therefore the assumption is made that the transverse strain in x-direction is equal to the strain in y-direction, and that the coefficient k is defined as the ratio between transverse strains and longitudinal strain induced solely by the external electric field, being:

$$k = \frac{\varepsilon_{11} \text{ (or } \varepsilon_{22})}{\varepsilon_{33}} \quad (9) \quad \text{and thus} \quad k = \frac{M_{13} \text{ (or } M_{23})}{M_{33}} \quad (10)$$

In literature through experiments it was found that the electromechanical coupling coefficient tensor M_{33} is not a material constant, but changes with increase or decrease of the electric field strength, as can be seen in figure 4. This means that in the model for each value of the electric field, the M_{33} value having lowest error to the experimental value for displacement has to be noted, instead of one constant M_{33} value for all electric field strengths.

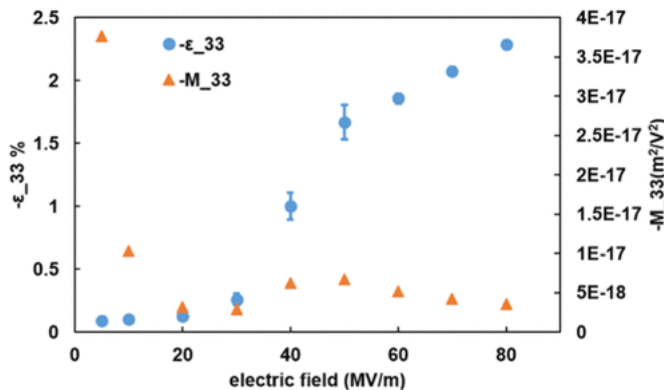


Figure 4. Measurements of longitudinal strain ϵ_{33} for different electric field strengths (0 to 80 MV/m) and the calculated coupling coefficient M_{33} for these electric field strengths.[5]

Since the setup of the electromechanical characterization experiment does not change between the types of samples, this assumption is valid for both the P(VDF-TrFE-CTFE) film and the P(VDF-TrFE-CTFE) nanofiber samples.

COMSOL Implementation - P(VDF-TrFE-CTFE) Film

Two FEA models of the P(VDF-TrFE-CTFE) material film are developed in the commercial FEA package COMSOL Multiphysics: one utilizing the COMSOL Electrostriction Multiphysics and Electromechanical Forces Multiphysics Modules within the programme, and the other utilizing the Shell Module. All three models are displayed in figure 5. The guide to creating each FEA model is included in the appendix.

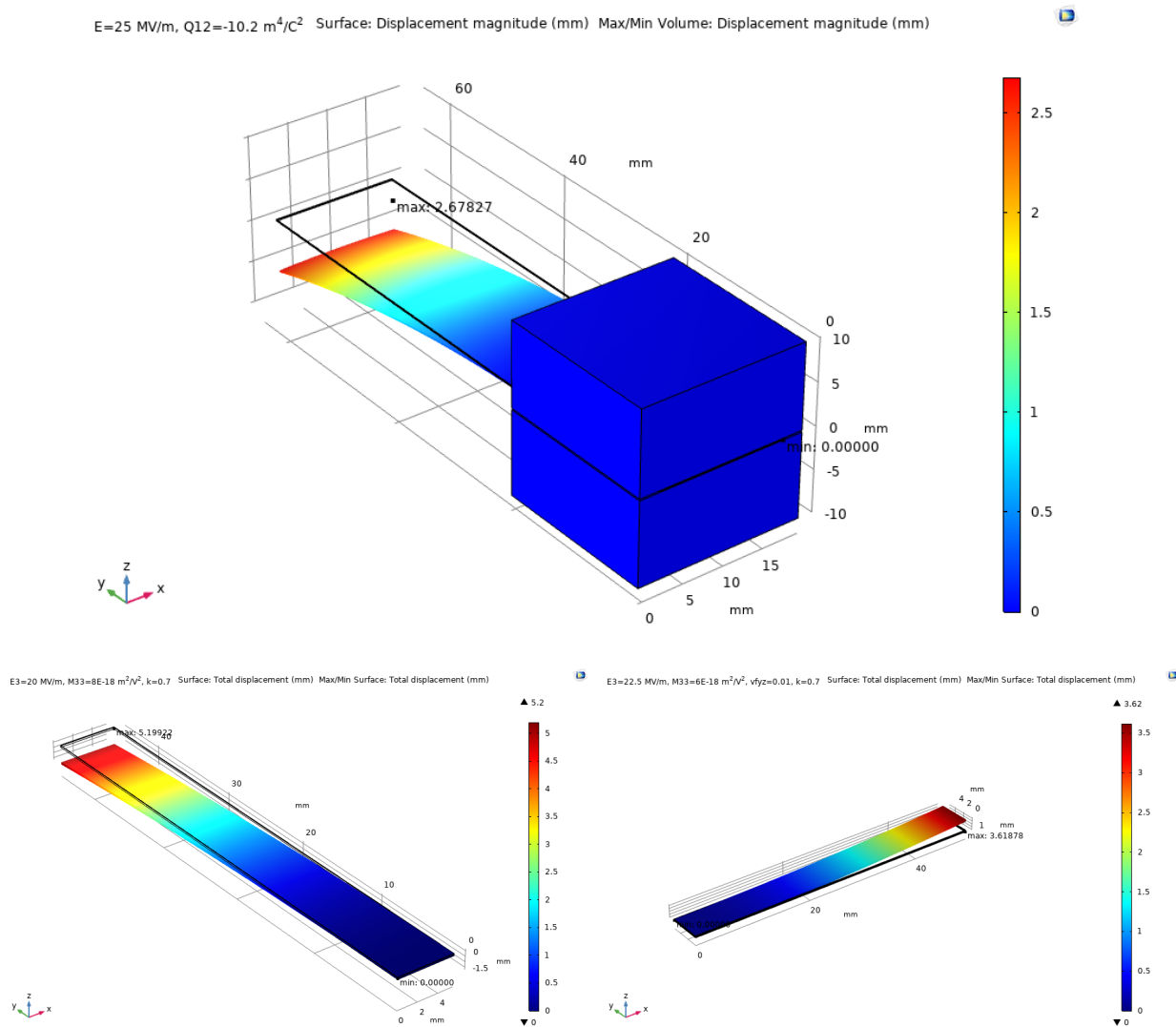


Figure 5. The three types of FEA models developed in this study. Top: Electrostriction Module Model, bottom left: Shell Module, bottom right: Aligned Nanofiber Shell Module.

Each FEA model has its pros and cons, hence both are used in the first part of this study for modelling and simulating the P(VDF-TrFE-CTFE) films.

The reason to use the Multiphysics Modules is that it allows for a complete, structured and stable intertwining of the electrical and the mechanical domain. The module that COMSOL provides does not have to be altered in any way, the parameters required only have to be filled in properly. The cons of using these Multiphysics Modules is the necessity to follow the module equations, requiring parameters of difficult estimation for the electrospun nanofibers, and the computational time required to do the computations.

Therefore, a model using the Shell Module in COMSOL is also created. The shell theory is a good approximation for the deformation of thin structures. By neglecting the normal and shear stresses in the zz-direction of the material, through the thickness, the shell elements assume a plane stress condition and do not have nodes in the zz-direction, which decreases the total number of nodes, decreasing the degrees of freedom in the model.[5] Although at first it does not seem like one structural mechanics module is able to connect the electrical domain to the mechanical domain, by modifying the constitutive equations of the shell elements according to equation (5), the electromechanical coupling stress terms are added to the original mechanical stress-strain equations, specifically the membrane components of second Piola-Kirchhoff stresses in xx-, yy-, and zz-directions with respect to the local coordinate system in COMSOL's Shell Module.[5] These additions to the constitutive equations come with additional instabilities to the model however, but lower the amount of parameters needed and the computational time marginally with respect to the Electrostriction Multiphysics Module.

$$\sigma_1 = (\lambda + 2\mu)\varepsilon_1 + \lambda\varepsilon_2 + \lambda\varepsilon_3 - [(\lambda + 2\mu)M_{13} + \lambda(M_{23} + M_{33})]E_3^2$$

$$\sigma_2 = (\lambda + 2\mu)\varepsilon_2 + \lambda\varepsilon_1 + \lambda\varepsilon_3 - [(\lambda + 2\mu)M_{23} + \lambda(M_{13} + M_{33})]E_3^2$$

(11)

$$\sigma_3 = (\lambda + 2\mu)\varepsilon_3 + \lambda\varepsilon_2 + \lambda\varepsilon_1 - [(\lambda + 2\mu)M_{33} + \lambda(M_{23} + M_{13})]E_3^2$$

COMSOL Implementation - P(VDF-TrFE-CTFE) nanofiber integrated PDMS mat

For the P(VDF-TrFE-CTFE) nanofiber integrated PDMS mat only one FEA model is made using the Shell Module. Because the P(VDF-TrFE-CTFE) nanofiber integrated PDMS mat is a composite material and can be seen as an transverse isotropic material, this would add obscure parameters to the model using the Electrostriction and Electromechanical Forces Multiphysics Modules. The use of these parameters is avoided in the shell module, hence it is a better candidate for trying to model the experimental test setup. Just as in the model for the P(VDF-TrFE-CTFE) film utilizing the Shell Module, the electrical domain and the mechanical domain have to be connected by modifying the constitutive equations of the shell elements. Since the nanofiber integrated mat classifies as an transverse isotropic material rather than an isotropic material, instead of modifying the membrane components of second Piola-Kirchhoff stresses in xx-, yy-, and zz-directions with respect to the local coordinate system in COMSOL's Shell Module as in equation (11), the equations are modified using Hooke's Law the stiffness matrix for transverse isotropic materials, as in equation (12).

$$\sigma_t = \frac{E(\lambda - v_v^2)}{(\lambda - \lambda v_H - 2v_v^2)(1 + v_H)} \epsilon_1 + \frac{E(\lambda v_H + v_v^2)}{(\lambda - \lambda v_H - 2v_v^2)(1 + v_H)} \epsilon_2 + \frac{v_v E}{(\lambda - \lambda v_H - 2v_v^2)} \epsilon_3 - \left[\frac{E(\lambda - v_v^2)}{(\lambda - \lambda v_H - 2v_v^2)(1 + v_H)} M_{13} + \frac{E(\lambda v_H + v_v^2)}{(\lambda - \lambda v_H - 2v_v^2)(1 + v_H)} M_{23} + \frac{v_v E}{(\lambda - \lambda v_H - 2v_v^2)} M_{33} \right] E_3^2 \quad (12)$$

$$\sigma_a = \frac{v_v E}{(\lambda - \lambda v_H - 2v_v^2)} \epsilon_1 + \frac{v_v E}{(\lambda - \lambda v_H - 2v_v^2)} \epsilon_2 + \frac{(1 - v_H)E}{(\lambda - \lambda v_H - 2v_v^2)} \epsilon_3 - \left[\frac{v_v E}{(\lambda - \lambda v_H - 2v_v^2)} M_{13} + \frac{v_v E}{(\lambda - \lambda v_H - 2v_v^2)} M_{23} + \frac{(1 - v_H)E}{(\lambda - \lambda v_H - 2v_v^2)} M_{33} \right] E_3^2$$

The equation σ_t is the equation implemented in both directions forming the transverse plane, since these two directions are equal because of isotropicity. The equation σ_a is implemented in the axis of symmetry, the direction of alignment of the nanofibers.

For the model for the P(VDF-TrFE-CTFE) nanofiber integrated PDMS mat, there is only studied if the model simulates a good approximation of the experimental results for a constant value of the electromechanical coefficient M_{33} and 1 chosen constant of k.

4. Results

Experimental results: Mechanical Characterization

The mechanical properties of the 3 samples determined by the mechanical characterization or found in literature are shown in table 3.

Sample	Sample 5 / Sample 6	Nanofiber Sample
Young's Modulus	0.095 [GPa]	Nanofiber Axial: 53 [MPa] Nanofiber Transverse: 4 [MPa] PDMS Matrix: 0.795879 [MPa]
Poisson's ratio	0.22	Nanofiber XY: 0.27 Nanofiber YZ: 0.01 PDMS Matrix: 0.49
Density	1500 [kg/m ³]	Nanofiber: 4.612E-4 [g/mm ³] PDMS Matrix: 965 [kg/m ³]
Shear Modulus	--	Nanofiber XY: 0.5 [GPa] PDMS Matrix: 250 [kPa]

Table 3. Relevant mechanical properties of the P(VDF-TrFE-CTFE) material and PDMS matrix in the 3 samples.

From this table, it can be observed that the nanofiber sample possesses completely different mechanical properties from the isotropic P(VDF-TrFE-CTFE) material used for the film in sample 5 and 6. This makes the nanofiber sample distinctly different from the isotropic film in every for this study relevant property.

Experimental Results: Electromechanical Characterization: Tip displacement

The readings for the tip displacement for the 3 different samples were inserted in a graph (figure 6). Since the electric polarization density and strain as well as the electric field strength and

mechanical strain were found to be coupled quadratically, a second degree polynomial trendline was made for each sample to check for this relation. The R-squared values are noted in table 4.

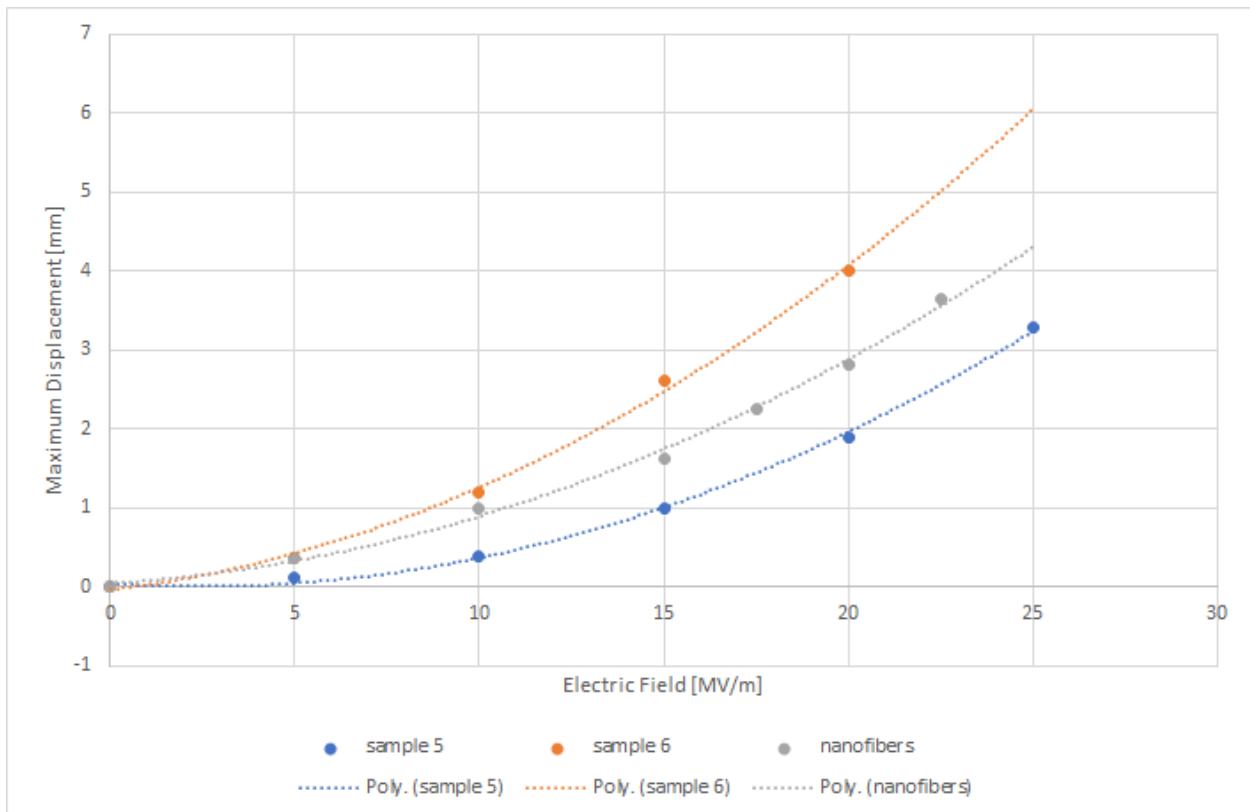


Figure 6. Maximum Tip Displacement of the P(VDF-TrFE-CTFE)-based actuators stimulated by different electric field strengths, including a second degree polynomial trendline.

Sample	R-squared
Sample 5	0.9984
Sample 6	0.997
Nanofiber Sample	0.9962

Table 4. R-squared values of the trendlines to the tip displacement data.

It is found that the R-squared values for all three displacement data curves show that all three the samples significantly follow the theoretical quadratic coupling of the electric polarization density or the electric field strength to mechanical strain. This means all samples closely resemble a second order polynomial and are therefore suitable to be modelled precisely by the two modules using quadratic coupling methods.

Modelling Results - Electrostriction Module Model
Sample 5

The results for the maximum volume displacement of the active layer of the sample 5 actuator for different values of Q12 at different electric field strengths are included in the appendix. For every electric field strength and every value for Q12 the error between the modelled displacement and the experimentally determined displacement was normalized, and for each value of Q12 the mean normalized error was calculated for all electric field strengths, the 4, 3 and 2 highest values of electric field and displayed in a graph (figure 7). The lowest values for the mean normalized errors between the experiment and the model and the corresponding values for Q12 are displayed in table 5. In figure 8, a comparison between the experimental maximum displacement values for and the modelled maximum displacement values for Q12=-10.2, Q12=-9.8 is displayed.

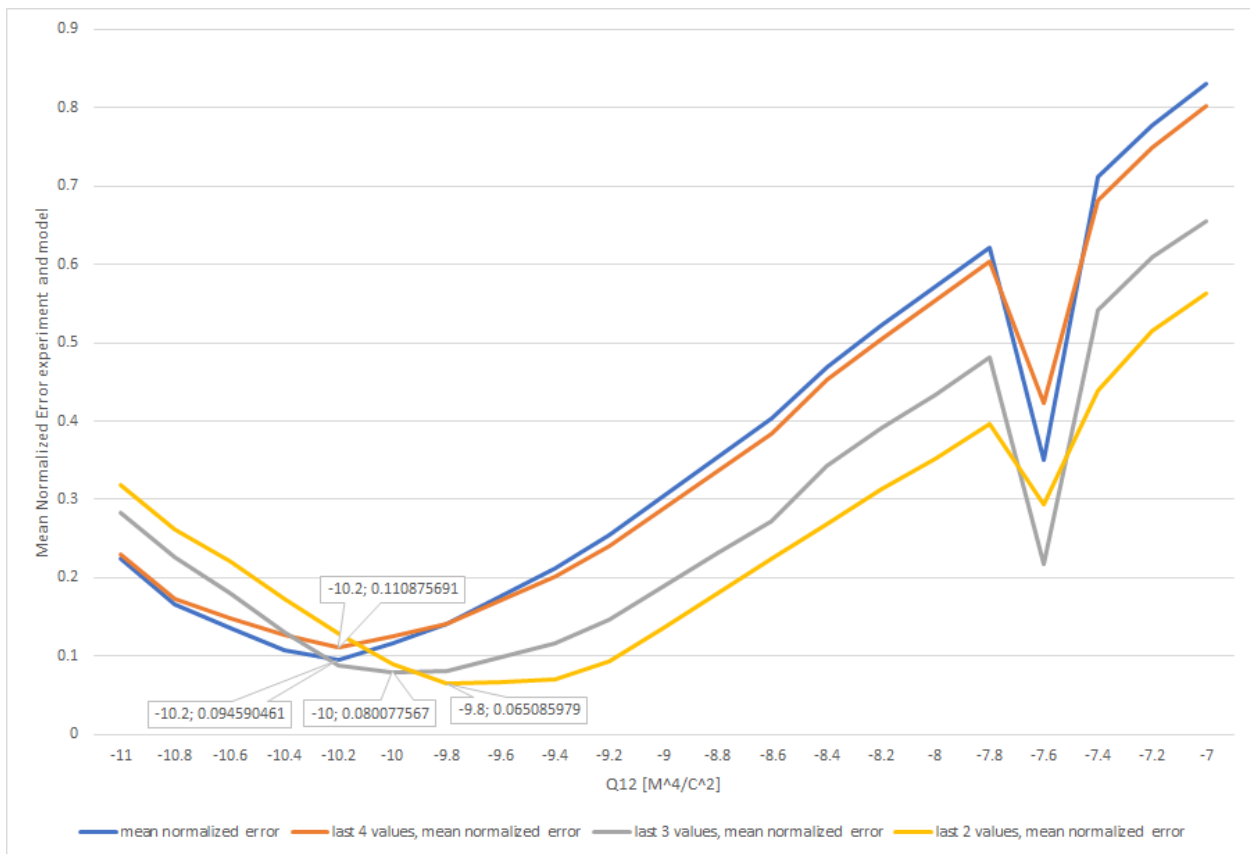


Figure 7. The mean normalized difference between the maximum displacement recorded in the experiment (sample 5) and the displacement simulated by the Electrostriction Module Model for different values of electrostrictive coefficient Q12 for all electric field strength measurements (blue), the last 4 values (orange), the last 3 values (grey) and the last 2 values (yellow).

Data name	Mean normalized error value	Q12 value
Mean normalized error	0.094590461	-10.2
Last 4 values, mean normalized error	0.110875691	-10.2
Last 3 values, mean normalized error	0.080077567	-10

Last 2 values, mean normalized error	0.065085979	-9.8
--------------------------------------	-------------	------

Table 5. The mean normalized errors between the experimental displacement data (sample 5) and the modelled displacement and the corresponding values of Q12.

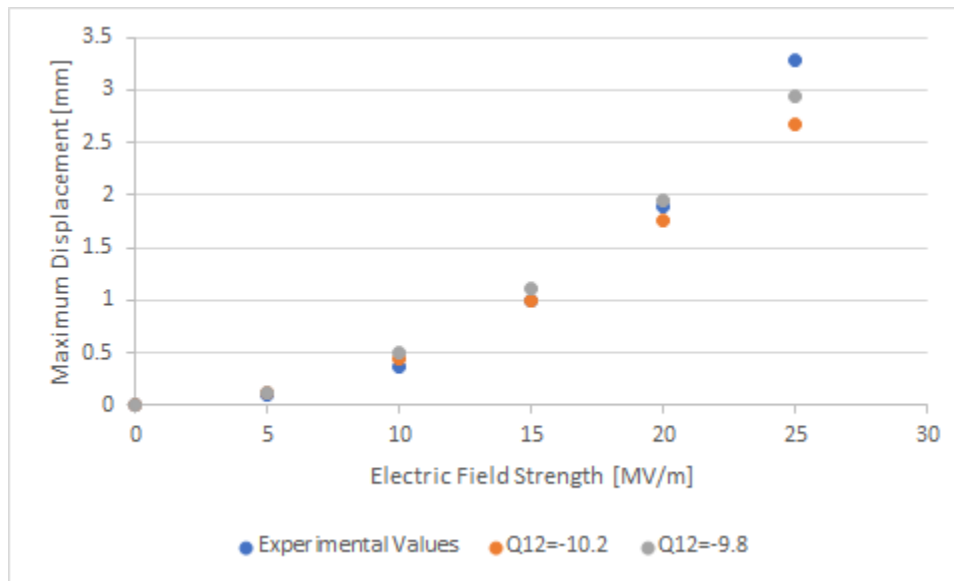


Figure 8. A comparison between the experimental recorded maximum displacement of sample 5 and the modelled maximum displacement of the electrostriction model of sample 5 for the value of Q12 with the lowest mean normalized error of all electric field measurements ($=-10.2$) and for the value of Q12 with the lowest mean normalized error of the 2 highest electric field strengths ($=-9.8$).

The Q12 value for which the mean normalized error is the smallest lies in the electric field range 0-25 MV/m around $-10 \text{ M}^4/\text{C}^2$ for sample 5. When all measurements are used the value of Q12= -10.2 . It can be noted that when the lower electric field strengths (5 MV/m, 10 MV/m and 15 MV/m) are dropped from calculating the mean normalized error, the ideal value for Q12, with the lowest mean error, shifts slightly to the right (to Q12= -9.8). Since the quadratic behaviour of the electrostriction becomes more outspoken with higher values of electric fields, this shift shows that there is still not a definitive answer to the Q12 value of sample 5. Instead, it is possible to assign a range to it, for these results being $[-10.2, -9.8]$. The true value of the Q12 coefficient of P(VDF-TrFE-CTFE) film sample 5 does not have to lie within this range. It is expected that for much higher electric field strengths, the value of Q12 for which the model approximates the experimental data best is even more shifted to the right. Since the values of Q12 ranging from -10 to -9.2 show a mean normalized error of less than 0.1 it is expected that the true value for the Q12 coefficient is within this range.

The results for Q12 = -7.6 are not following the increasing mean normalized error trend and are therefore labelled as unreliable results.

Sample 6

The results for the maximum volume displacement of the active layer of the sample 6 actuator for different values of Q12 at different electric field strengths are included in the appendix. For every electric field strength and every value for Q12 the error between the modelled

displacement and the experimentally determined displacement was normalized, and for each value of Q12 the mean normalized error was calculated for all electric field strengths, the 3 and 2 highest values of electric field and displayed in a graph (figure 9). The lowest values for the mean normalized errors between the experiment and the model and the corresponding values for Q12 are displayed in table 6. In figure 10, a comparison between the experimental maximum displacement values for and the modelled maximum displacement values for Q12=-10.2, Q12=-9.8 is displayed.

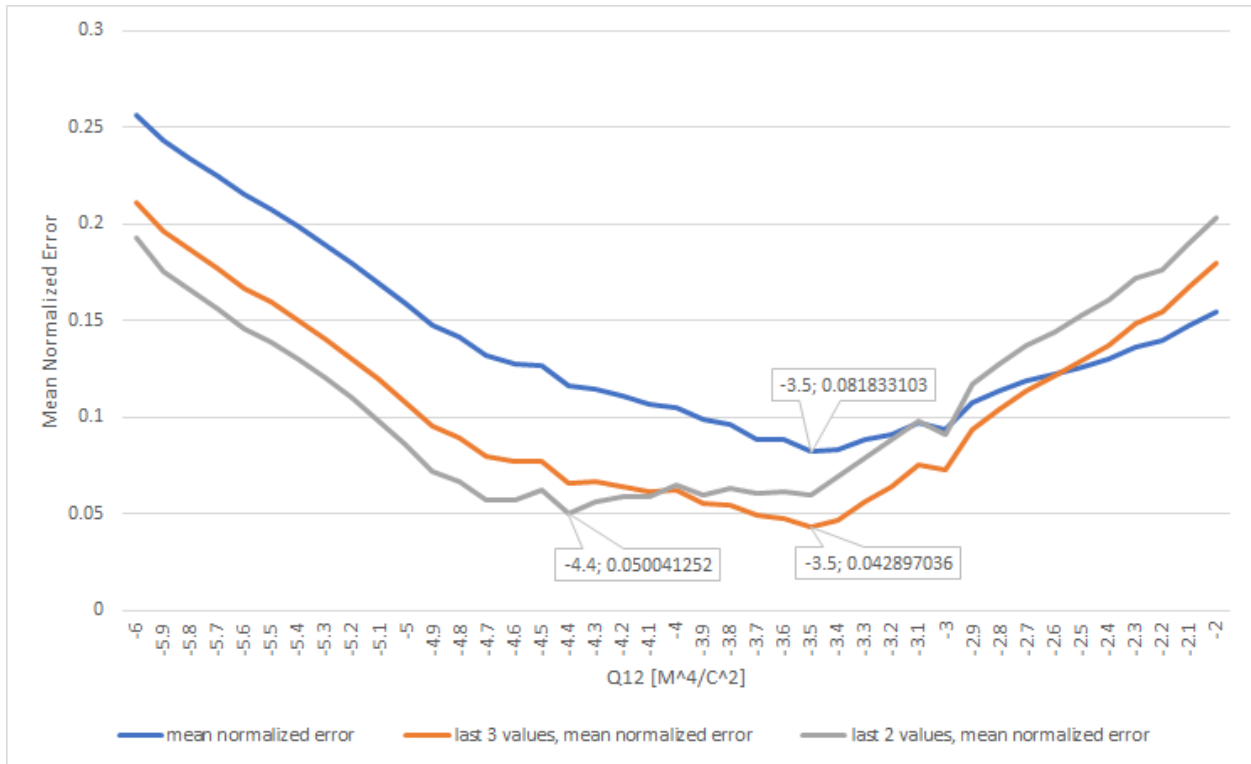


Figure 9. The mean normalized difference between the maximum displacement recorded in the experiment (sample 6) and the displacement simulated by the Electrostriction Module Model for different values of electrostrictive coefficient Q12 for all electric field strength measurements, the last 3 values and the last 2 values.

Data name	Mean normalized error value	Q12 value
Mean normalized error	0.081833103	-3.5
Last 3 values, mean normalized error	0.042897036	-3.5
Last 2 values, mean normalized error	0.050041252	-4.4

Table 6. The mean normalized errors between the experimental displacement data (sample 6) and the modelled displacement and the corresponding values of Q12.

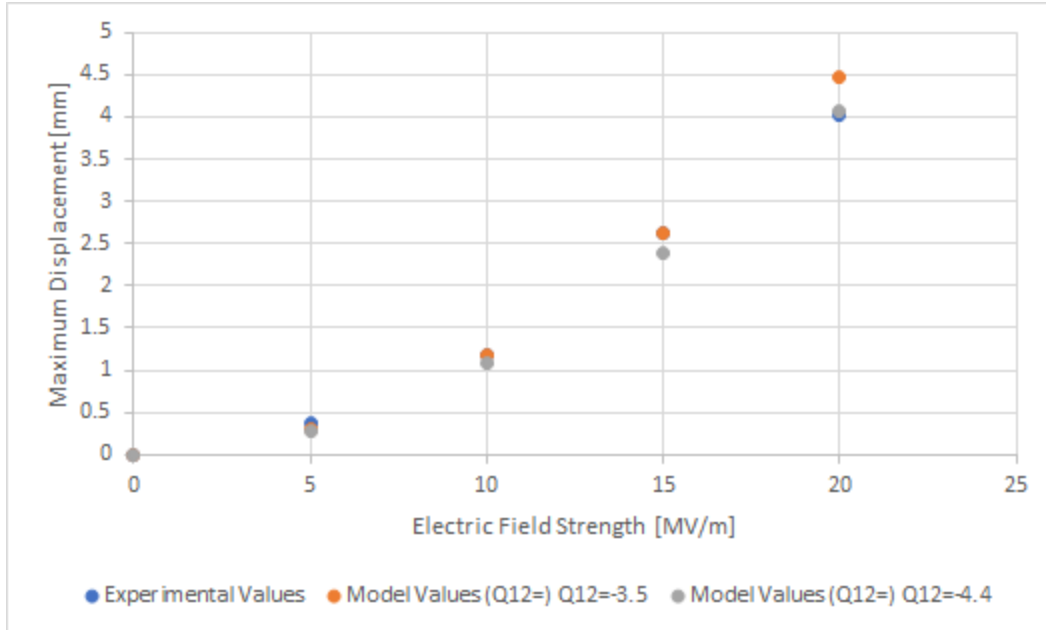


Figure 10. A comparison between the experimental recorded maximum displacement of sample 6 and the modelled maximum displacement of the electrostriction model of sample 6 for the value of Q12 with the lowest mean normalized error of all electric field measurements ($=-3.5$) and for the value of Q12 with the lowest mean normalized error of the 2 highest electric field strengths ($=-4.4$).

The Q12 value for which the mean normalized error is the smallest lies in the electric field range 0-25 MV/m around $-3.5 \text{ M}^4/\text{C}^2$ for sample 6. It can be noted that when the lower electric field strengths (5 MV/m and 10 MV/m) are dropped from calculating the mean normalized error, more emphasising on the quadratic coupling between the electric polarization density and the strain, the ideal value for Q12, with the lowest mean error, shifts to the left. This means that the Q12 value for sample 6 for these results lies somewhere along a certain range. The true value of Q12 of sample 6 does not have to lie within that range. It is expected that the true value of Q12 for sample 6 lies within the range $[-5, -3.5]$, based on the values of Q12 for which the normalized mean error for only the last 2 electric field values is lower than 0.1, between -5.1 and -3 , and based on the given that the Q12 value including all electric field strengths is -3.5 and shifts to the left when the lower electric field strengths are excluded from the calculation.

Samples 5 and 6

Both samples could be approximated using the Electrostriction Module Model, but the behaviour of the models was found to be different from each other. The ranges for the values of Q12 do not overlap between the samples. Because the active layers in both samples are not identical, this is most likely explained by the difference in spatial dimensions between the two samples. The model is verified by the small mean normalized error value between the experimental data and the modelled results of the two samples. Moreover, some differences in the experimental results are due to a voltage drop on the electrodes, due to imperfections of the gold sputtered electrodes that are different in the two samples. This is not considered in the model and is left for future work. However, the manipulation of the electrostrictive coefficient is an effective way to consider the imperfections of the fabrication process in the model and therefore to obtain a

suitable model for both the samples. The model is verified by the small mean normalized error value between the experimental data and the modelled results of the two samples.

Modelling Results - Shell Module Model

Sample 5

The complete results for the maximum surface displacement of the active layer of the sample 5 actuator for different values of the ratio between the transverse strains and the longitudinal strain k for different values for the electromechanical coupling coefficient M_{33} at different electric field strengths are included in the appendix. For every electric field strength and a range of M_{33} values the value of M_{33} which fitted the experimental data best was noted. For each value of k these M_{33} values were put in a graph to display the behaviour of the coefficient (figure 11). In figure 12, for $k=0.7$ the displacement values belonging to the best fitting M_{33} values are compared to the experimental values of sample 5.

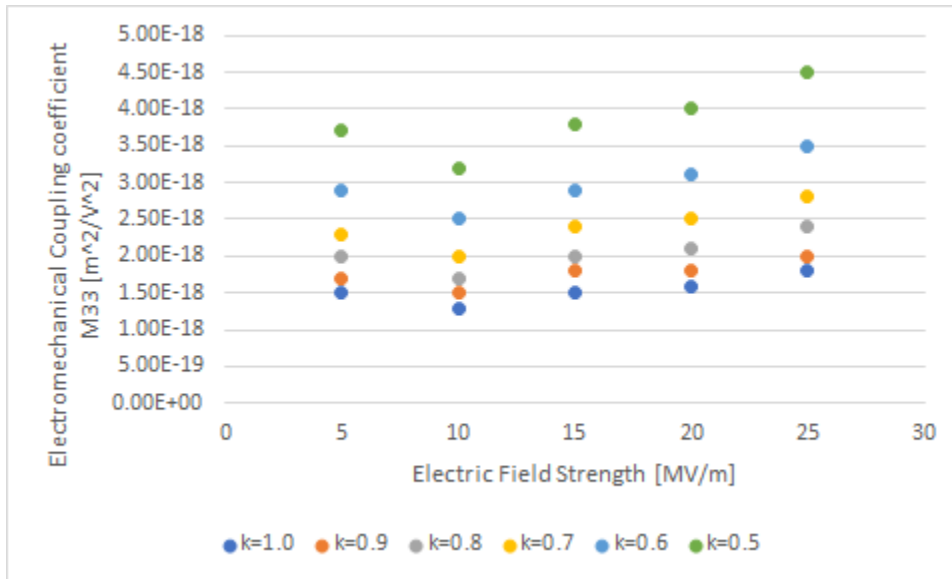


Figure 11. Electromechanical coupling coefficient M33 values for best fitting the model to the sample 5 for different values of k , the ratio between transverse strains and longitudinal strain.

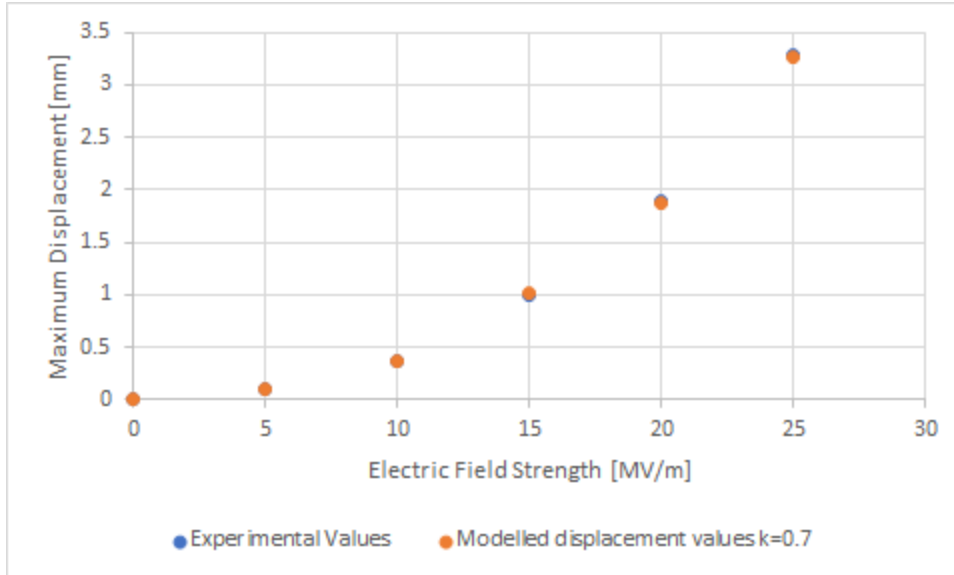


Figure 12. A comparison between the experimentally recorded displacement values and the modelled displacement values for $k=0.7$ of sample 5.

Looking at figure 11 it can be noted that for each value of k , the electromechanical coupling coefficient M_{33} follows a similar pattern in the tight electric field strength window worked in. First the value of M_{33} decreases when the electric field strength is increased from 5 MV/m to 10 MV/m, before increasing when the electric field is further increased to 15 MV/m, 20 MV/m and 25 MV/m. Figure 12 shows that the assigning of the most perfect value of M_{33} causes the modelled displacement values to almost have no difference from the experimental values.

Sample 6

The complete results for the maximum surface displacement of the active layer of the sample 5 actuator for different values of the ratio between the transverse strains and the longitudinal strain k for different values for the electromechanical coupling coefficient M_{33} at different electric field strengths are included in the appendix. For every electric field strength and a range of M_{33} values the value of M_{33} which fitted the experimental data best was noted. For each value of k these M_{33} values were put in a graph to display the behaviour of the coefficient (figure 13). In figure 14, for $k=0.7$ the displacement values belonging to the best fitting M_{33} values are compared to the experimental values of sample 5.

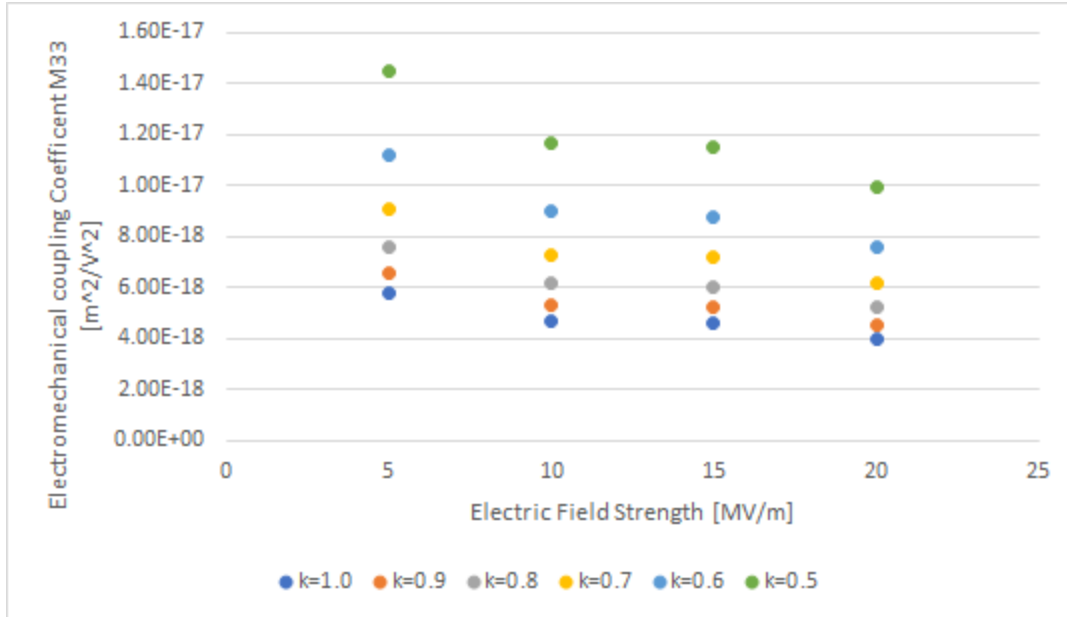


Figure 13. Electromechanical coupling coefficient M_{33} values for best fitting the model to the sample 6 for different values of k , the ratio between transverse strains and longitudinal strain.

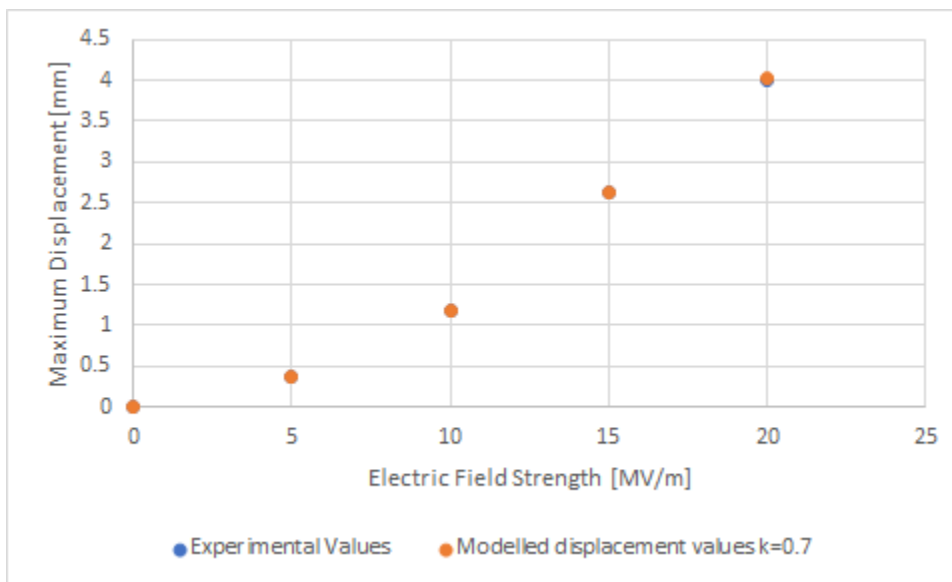


Figure 14. A comparison between the experimentally recorded displacement values and the modelled displacement values for $k=0.7$ of sample 6.

Looking at figure 13 it can be noted that for each value of k , the electromechanical coupling coefficient M_{33} follows a similar pattern in the tight electric field strength window worked in. The value of M_{33} decreases gradually when the electric field strength is increased. Figure 14 shows that the assigning of the most perfect value of M_{33} causes the modelled displacement values to almost have no difference from the experimental values.

Sample 5 and 6

Both samples could be approximated using the Shell Module Model, but not much can be said about the behaviour of the models. Sample 5 at first shows a slight decrease when the electric field strength is increased from 5 MV/m to 10 MV/m. A further increase of the electric field strength causes an increase of M_{33} . Sample 6 on the other hand demonstrates a slight decrease in the M_{33} value when the electric field strength is increased.

Modelling Results - Nanofiber Sample

For the nanofibers, it was only investigated if the model would be able to give a good approximation of the tip displacement at a fixed value of M_{33} for a fixed value of k. These values are $M_{33} = 6E-18 \text{ m}^2/V^2$ and $k=0.7$. The value for k was chosen based on the best fitting value for k found in the article of Zhang et al. (2018) [5], that is also in good agreement with the simulation results. A comparison of these results is shown in table 7 and visualized in figure 15.

Electric Field	Experimental results	M33=6E-18, k=0.7
0 MV/m	0	0
5 MV/m	0.37	0.1787
10 MV/m	1	0.71482
15 MV/m	1.63	1.60835
17.5 MV/m	2.26	2.18914
20 MV/m	2.82	2.85928
22.5 MV/m	3.64	3.61878

Table 7. Comparison between the experimental results on the nanofiber sample and the modelled results of the nanofiber model with fixed M33 (=6E-18) and k (=0.7) values.

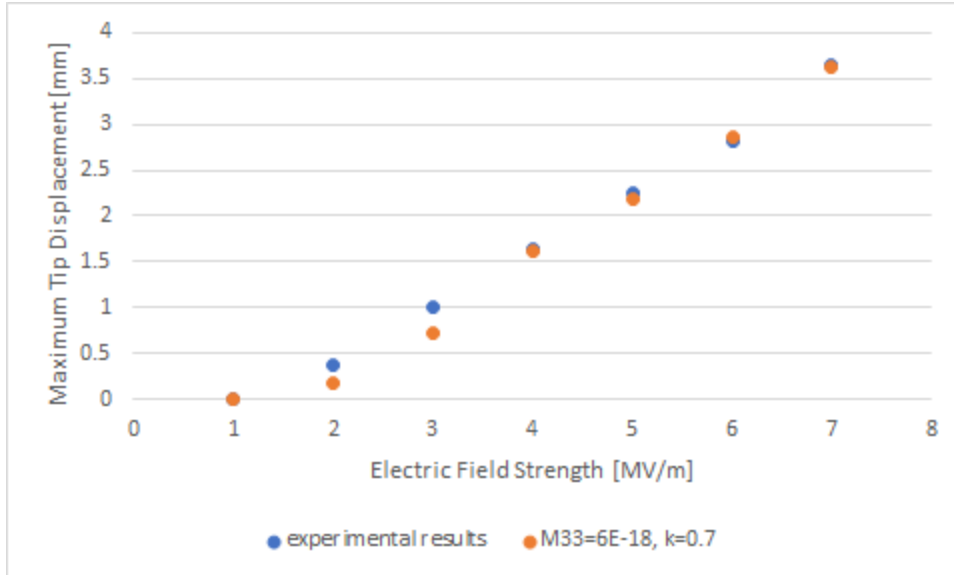


Figure 15. Comparison between the experimental results on the nanofiber sample and the modelled results of the nanofiber model with fixed values for M33 (=6E-18) and k (=0.7).

Figure 15 shows that the modelled results better model the experimental results at higher electric field strengths (15 MV/m - 22.5 MV/m). At lower electric fields the relative error between the experimental results and the modelled results is higher. This might be explained by the low impact of the quadratic coupling of the electric field to the mechanical strain. Thus, at low electric fields, the impact of this coupling is lower than at higher electric fields. Overall the model is capable of recreating the experimental results with the predetermined settings.

5. Discussion

The objective of this study has been to be able to simulate the electrostrictive behaviour of P(VDF-TrFE-CTFE) through different methods of modelling to get a better understanding of the coupled behaviours of EAPs. Through this study a good balance between experimental data and FEA results is achieved.

The results from the experimental test setup recording the electromechanical response of the active material in the form of maximum tip displacement results showed that all three samples closely resemble a second degree polynomial trend ($R > 0.995$ for all samples), as is theoretically expected for electro-active materials with electrostrictive properties. This shows the way the actuator samples are manually fabricated is very refined and that the experimental test setup is excellent for performing electromechanical characterizations of EAPs coming in different forms, e.g. homogeneous films and nanofiber integrated mats. The fabrication methods and test setup could both be adopted by others for convenient EAP sample fabrication and electromechanical characterization.

The developed model utilizing the Electrostriction Module has shown to be able to approximate the experimental data of an isotropic P(VDF-TrFE-CTFE) film by varying one specific parameter, being the Electrostrictive Q-matrix element Q12. For both sample 5 and sample 6, the model could be validated with the experimental data. Since Q12 was not equal in both samples and was also not experimentally obtained, but only used as a variable in the

Electrostriction Module model, a next step in validating the model should be gathering experimental data on the Q12 coefficient of film samples to be able to investigate the behaviour of this electrostrictive Q-matrix element. This would be a first in the field but being able to understand these interdomain properties will help greatly in understanding the behaviour EAPs.

The Electrostriction Module model has been specifically developed to study the electrostrictive behaviour of the P(VDF-TrFE-CTFE) material in the EAP more closely, since it treated electrostriction as a separate electromechanical response, separated from the Maxwell stress. However the model has shown to require more computational power and time than other models modelling the electromechanical responses of EAPs in literature. This, combined with the amount of input data needed for the model to be able to work, would make it subordinate to the already existing models. However, this model is yet to be completely discovered and, with this study being a first attempt at modelling the behaviour of an EAP, there is still plenty of room left to improve this model. The importance of the full electrostrictive Q-matrix for anisotropic materials has not yet been uncovered and a refining of the system settings could lower the computational time significantly to make the model competitive.

The second model, utilizing the Shell Module, predeveloped in an earlier study by Zhang et al. (2018) showed to also be as good in modelling the electrostrictive behaviour of an isotropic P(VDF-TrFE-CTFE) film. The model was again validated by the experimental results. The behaviour of the electromechanical coefficient M_{33} could not completely be followed as the behaviour of the curves from sample 5 and 6 are not alike and do also not closely resemble the experimentally derived curve found by Zhang et al. (2018) [5]. A future step is providing additional validation of the model by experimentally deriving the M_{33} coefficient for the applied electric field strengths like done the referenced study of Zhang et al. (figure 3). This allowed them to easily validate the model and investigate the best fitting ratio between the transverse strains and the longitudinal in the parameter k. M_{33} could be experimentally derived by measuring the longitudinal strain for different electric field stimulations and subsequently calculating the corresponding M_{33} values.

The adaptations made to make the model suitable for modelling the nanofiber integrated mat sample showed to be able to approximate the experimental data for fixed values of M_{33} (=6E-18) and k (=0.7). Taking into account the assumptions made regarding the approximation of the Poisson's ratio of the nanofiber integrated mat and the theories used to assess the composite material (i.e. transverse isotropy combined with mixture theory), this model still shows to be a very fine approximation of the experimental results. For further studies it is important that assumptions are replaced by experimental data to provide further support for those used assumptions and theories and for the validation of the model. A method on how to determine the poisson's ratio of the nanofibers in the plane of symmetry would be of great assistance and the introduction of a factor grading the level of alignment of the nanofibers in the PDMS matrix would increase the level of preciseness of the model. And there are many more methods to further increase the accuracy of this first model.

Looking at the results from this study, not much can be said about the influence the organization of the P(VDF-TrFE-CTFE) material in electrospun aligned nanofibers has on the electromechanical coupling coefficient M_{33} based on the results of the electromechanical

characterization and the modelling of the samples. The three samples, sample 5, sample 6 and the nanofiber sample, vary in too many different properties (i.e. spatial dimensions, build-up of the sample, imperfections) from each other to be able to conclude any statistical differences between them. In further research, trying to create samples differing in as few properties, same materials, same spatial dimensions, different structured organization, can help find statistically significant differences between the unorganized film sample and the organized aligned nanofiber sample.

In order to understand EAPs using the Shell Module model, further research regarding the M_{33} coupling coefficient, further dissecting it in a Maxwell stress component and an electrostriction component, as is done for deriving the strain for the Electrostriction and Electromechanical Forces in equation (3). This would assist in clearing up more questions about how the coupling coefficient might be changed when the structure of the material is altered and at which component, electrostriction or Maxwell stress, that change would mostly be present.

Lastly, the mixture theory has shown to be an excellent theoretical model for the nanofiber sample in the approximation of mechanical properties of the nanofiber integrated composite material. It could therefore be further used to start investigating the ideal nanofiber-to-matrix element ratio in the EAP composite with regards to desired mechanical and electromechanical properties in future research.

6. Conclusion

The fabrication process of the EAP samples and the experimental test setup for the electromechanical characterization of the samples used for this study are already very refined as the samples show to follow the theoretical quadratic coupling and are therefore very suitable for modelling using the two modelling methods used in this study.

Both methods of modelling were able to recreate the coupled responses of the P(VDF-TrFE-CTFE) film samples and the model using the Shell Module was also able to recreate the coupled response of the P(VDF-TrFE-CTFE) nanofiber integrated PDMS sample. To model the P(VDF-TrFE-CTFE) material, either the electrostrictive coupling tensor or the electromechanical coupling tensor is implemented in the stress-strain relation. In one model this was done via a specific module available in the FEA modelling software, in the other this was made possible by adding it in an electromechanical term in the constitutive equations. The FEA results showed to be very similar to the experimental results for the different samples with the right settings. The model utilizing the Shell Module shows to be a good method for recreating the behaviour of more complicated structures (i.e. integrated nanofibers). To see if the other model is, too, capable of recreating the behaviour for such structures and can be improved, further research is needed. After the validation by experimental results, we conclude that all three FEA models developed in this article can recreate the behaviour of the bending behaviour of EAPs.

Declaration of conflicting interests

The author declared no potential conflicts of interest with the respect to the research, authorship, and/or publication of this article.

References

- [1] Jabareen, M. (2015). On the Modeling of Electromechanical Coupling in Electroactive Polymers Using the Mixed Finite Element Formulation. *Procedia IUTAM*, 12, 105–115. <https://doi.org/10.1016/j.piutam.2014.12.012>
- [2] Ahmed, S., & Ounaies, Z. (2016). A study of metalized electrode self-clearing in electroactive polymer (EAP) based actuators. *Electroactive Polymer Actuators and Devices (EAPAD) 2016*, 9798, 97983F. <https://doi.org/10.1117/12.2222135>
- [3] Lam, T. N., Ma, C. Y., Hsiao, P. H., Ko, W. C., Huang, Y. J., Lee, S. Y., Jain, J., & Huang, E. W. (2021). Tunable Mechanical and Electrical Properties of Coaxial Electrospun Composite Nanofibers of P(VDF-TrFE) and P(VDF-TrFE-CTFE). *International Journal of Molecular Sciences*, 22(9). <https://doi.org/10.3390/ijms22094639>
- [4] D'Anniballe, R., Zucchelli, A., & Carloni, R. (2021). Towards Poly(vinylidene fluoride-trifluoroethylene-chlorotrifluoroethylene)-Based Soft Actuators: Films and Electrospun Aligned Nanofiber Mats. *Nanomaterials (Basel, Switzerland)*, 11(1), 172. <https://doi.org/10.3390/nano11010172>
- [5] Zhang, W., Ahmed, S., Masters, S., Hong, J., Ounaies, Z., & Frecker, M. (2018). Finite element analysis of electroactive and magnetoactive coupled behaviors in multi-field origami structures. *Journal of Intelligent Material Systems and Structures*, 29(20), 3983–4000. <https://doi.org/10.1177/1045389X1880>
- [6] Poncet, P., Casset, F., Latour, A., Dos Santos, F. D., Pawlak, S., Gwoziecki, R., Devos, A., Emery, P., & Fanget, S. (2017). Static and dynamic studies of electro-active polymer actuators and integration in a demonstrator. *Actuators*, 6(2), 2–11. <https://doi.org/10.3390/act6020018>
- [7] Zhang, Y., Perrin, V., Seveyrat, L., & Lebrun, L. (2020). On a better understanding of the electromechanical coupling in electroactive polyurethane. *Smart Materials and Structures*, 29(5), 055007.
- [8] McGough, Kevin & Ahmed, Saad & Frecker, Mary & Ounaies, Zoubeida. (2014). Finite element analysis and validation of dielectric elastomer actuators used for active origami. *Smart Materials and Structures*. 23. 094002. 10.1088/0964-1726/23/9/094002.
- [9] Ahmed, S., Hong, J., Zhang, W., Kopatz, J., Frecker, M., & Ounaies, Z. (2018). Various design approaches to achieve electric field-driven segmented folding actuation of electroactive polymer (EAP) sheets. *May*, 71. <https://doi.org/10.1117/12.2309378>
- [10] Solvne ® T EAP Ferrorelaxor Polymer. (2017). 2017. (technical datasheet)
- [11] Hegemier, G. A., Gurtman, G. A., & Nayfeh, A. H. (1973). A continuum mixture theory of wave propagation in laminated and fiber reinforced composites. *International Journal of Solids and Structures*, 9(3), 395–414. [https://doi.org/10.1016/0020-7683\(73\)90088-7](https://doi.org/10.1016/0020-7683(73)90088-7)
- [12] Qiao, B., Wang, X., Tan, S., Zhu, W., & Zhang, Z. (2019). Synergistic Effects of Maxwell Stress and Electrostriction in Electromechanical Properties of Poly(vinylidene fluoride)-Based Ferroelectric Polymers. *Macromolecules*, 52(22), 9000–9011. <https://doi.org/10.1021/acs.macromol.9b01580>
- [13] Roland, C. M., Garrett, J. T., Casalini, R., Roland, D. F., Santangelo, P. G., & Qadri, S. B. (2004). Mechanical and Electromechanical Properties of Vinylidene Fluoride Terpolymers. *Chemistry of Materials*, 16(5), 857–861. <https://doi.org/10.1021/cm034822h>
- [14] Mentrasti, L., Molari, L., & Fabiani, M. (2021). Poisson's ratio bounds in orthotropic materials. Application to natural composites: wood, bamboo and *Arundo donax*. *Composites*

Part B: Engineering, 209(November 2020), 108612.

<https://doi.org/10.1016/j.compositesb.2021.108612>

[15] Gusev, A. A., Hine, P. J., & Ward, I. M. (2000). Fiber packing and elastic properties of a transversely random unidirectional glass/epoxy composite. *Composites Science and Technology*, 60(4), 535–541. [https://doi.org/10.1016/S0266-3538\(99\)00152-9](https://doi.org/10.1016/S0266-3538(99)00152-9)

[16] Epaarachchi, J. A. (2011). *The effect of viscoelasticity on fatigue behaviour of polymer matrix composites. Creep and Fatigue in Polymer Matrix Composites*, 492–513. doi:10.1533/9780857090430.3.492

[17] Li, F., Jin, L., Xu, Z., & Zhang, S. (2014). Electrostrictive effect in ferroelectrics: An alternative approach to improve piezoelectricity. *Applied Physics Reviews*, 1(1).

<https://doi.org/10.1063/1.4861260>

[18] Li, J, Rao, N (2004) Micromechanics of ferroelectric polymer-based electrostrictive composites. *Journal of the Mechanics and Physics of Solids* 52(3): 591–615.

[19] Newnham, RE, Sundar, V, Yimnirun, R. (1997) Electrostriction: nonlinear electromechanical coupling in solid dielectrics. *The Journal of Physical Chemistry B* 101(48): 10141–10150

[20] Popov, V. L., Heß, M., & Willert, E. (2019). In *Handbook of Contact Mechanics*. 1st Edition. Springer-Verlag Berlin Heidelberg. Berlin. <https://doi.org/10.1007/978-3-662-58709-6>

Appendix

1. Ethics Paragraph

1. Identification of the key ethical issues

A lot of ethical challenges in this research revolved around data. One of those challenges on data was the use of approximations instead of real data. Not every parameter or property value can be determined experimentally which means that we have to make assumptions to come up with a good approximation of these parameters and properties. This ultimately affects first the accuracy but can also affect the precision of the results, since multiple parameter and property assumptions and approximations can affect other parameters as well. It is important to find the golden mean between experimentally determinations and approximations. For creating all three models it has always been important to perform experiments on the mechanical properties and electromechanical response to gather data first. The model on the aligned electrospun nanofiber integrated PDMS mat required data input that was practically not possible to be obtained with the lab equipment we had at our disposal. Therefore, larger assumptions had to be made. During the assembling of these assumptions, we always tried to incorporate as much experimental data as possible. An example of this is the assigning of the transverse isotropic material model to our aligned nanofibers. By assuming the nanofibers to be aligned perfectly, we were able to use this theory to make it easier for ourselves to model the nanofibers. Had we not made this assumption we would not have been able to use this theory and would therefore find a more difficult method to approximate the experimental samples. Making assumptions in modelling is very much accepted in the field of EAPs. It is not possible to recreate the experiment environment in your model. In each model multiple assumptions are always done to make the modelling easier while also keeping the accuracy and precision of the model as high as possible.[1,2]

2. Societal impact: why is your research important? What is the added value for society?

The entire nature of the research can also be seen as an ethical challenge: what is the added value of a model recreating an earlier performed experiment if you already have the data from the experiments? How does that make my research important? Does it have any added value for society? Finite element analysis research is becoming more and more important in many different fields of interest, because being able to understand a material so well that you are able to model it, means that you wouldn't need to perform as much time consuming, expensive experiments anymore. Relying on physics-based, modelled results rather than experimentally obtained results, creates a lot more freedom when it comes to making decisions about what aspect of a setup to research. When only relying on experiments, often only a very specific case is studied, while with a model it is much easier to study more of such specific cases. In the case of my research, I have made a first step to understanding and further researching organized aligned electrostrictive nanofiber integrated composite mats. Experiments on these nanofiber structures will still be necessary to obtain more experimental data on the electrostrictive nanofibers, but the created model is a first attempt to structurally understand the electrostrictive nanofibers through physics-based mathematical modelling. Ultimately this will increase the speed of the research and allow for more freedom in the research.[3]

- [1] Bellenger, E., Benhafid, Y., & Troussier, N. (2008). Framework for controlled cost and quality of assumptions in finite element analysis. *Finite Elements in Analysis and Design*, 45(1), 25–36. doi:10.1016/j.finel.2008.07.002
- [2] Philip Drijber, F. L. I., Finlay, J. B., & Dempsey, A. J. (1992). Evaluation of linear finite-element analysis models' assumptions for external fixation devices. *Journal of Biomechanics*, 25(8), 849–855. doi:10.1016/0021-9290(92)90225-p
- [3] Bathe, K. J., & Saunders, H. (1984). Finite Element Procedures in Engineering Analysis. *Journal of Pressure Vessel Technology*, 106(4), 421–422. <https://doi.org/10.1115/1.3264375>

2. Electrostriction Module Film Model Guide

Introduction

In this file the process to create a model for an electrostrictive film using the electrostriction multiphysics in COMSOL is recorded. In this test setup, a film consisting of 1 electroactive layer and 1 passive layer is created, on the back side kept in place by 2 immovable block objects. On the top and bottom side the electroactive layer is sputtered with gold to create 2 opposing electrodes allowing for an electric field to be created.

COMSOL Model

In **Model Wizard**, select **3D**, then under **Structural Mechanics** select and add **Solid Mechanics (solid)** and in **AC/DC** under **Electric Fields and Currents** select and add **Electrostatics (es)**. In **Study** select **Stationary**.

In **Global Definitions**, set the parameters as shown in Table 1.

Name	Expression	Value	Description
E	15 [MV/m]	1.5E7 V/m	Electric Field strength
d	150E-6 [m]	1.5E-4 m	Distance between electrodes (thickness of the electroactive material)
Q11	-12 [m ⁴ /C ²]	-12 [m ⁴ /C ²]	Electrostrictive Q-matrix Coefficient Q11
Q12	-3.5 [m ⁴ /C ²]	-3.5 [m ⁴ /C ²]	Electrostrictive Q-matrix Coefficient Q12

Table 1. Model parameters in Parameters 1.

(Optional)

Set material property parameters for the electroactive material to avoid using build-in materials in COMSOL.

In **Geometry**, set **unit length** to **mm**. Create 4 **blocks** as shown in table 2. Form a **Union**.

Block #	Block 1	Block 2	Block 3	Block 4
Name	'Passive Layer'	'Active Layer'	'Upper immovable object'	'Lower immovable object'
Width	11	11	15	15
Depth	65	65	20	20
Height	0.057	d	10	10
[x,y,z] corner position	[4,0,0]	[4,0,0.057]	[2,0,-10]	[2,0,0.057+d]

Table 2. Dimensions and position of the blocks.

In **Materials**, select **add Material from Library**, add the following materials and assign them to the corresponding blocks with the correct properties, all shown in table 3.

Material	Block	Young's Modulus	Poisson's ratio	Density	Relative permittivity
Kapton H (Polyimide tape) [solid]	'Passive Layer'	8.46E08	0.34	1.42[g/cm ³]	-
Polyvinylidene fluoride (PVDF)	'Active Layer'	9.5E07	0.22	1.50[g/cm ³]	45
(C ₃ H ₄ O ₂) _n (Polylactic acid, PLA) (Bodurov et al. 2016: PDLA; n 0.405-0.635 μm)	'Upper immovable object' & 'Lower immovable object'	350E07	0.33	0.95[g/cm ³]	-

Table 3. Materials with material properties for the different blocks.

In **Solid Mechanics**, check if every block in the geometry is selected. Under **Domain Constraints** add **Fixed Constraints**. Select the Upper immovable object block and Lower immovable object block. Under **Boundaries** add **Fixed Constraint** and select the **back surface** (y=0) of both the Active Layer and Passive Layer.

In **Electrostatics**, only have the Active Layer block selected. Under **Charge Conservation 1**, change **Material Type** to **Solid**. Under **Initial Values 1**, change the **Electric potential** to V=0 V. Add **Electric Potential**. Change the Electric Potential to E*d. Add **Ground**. Select the surface connecting the Active Layer to the Passive Layer block.

In **Multiphysics**, add **Electromechanical Forces** and **Electrostriction**. Under **Electromechanical Forces**, couple **Solid Mechanics (solid)** to **Electrostatics (es)** and check if the **Active Layer block** is selected. Under **Electrostriction**, couple **Solid Mechanics (solid)** to **Electrostatics (es)**. Set Coupling Type to **Polarization contribution to strain** and set Electrostrictive strain tensor to **Quadratic**, Solid model to **Isotropic** and specify as **Electrostrictive Q-matrix components**. For Q11 and Q12 fill in parameters **Q11** and **Q12** respectively.

In **Mesh**, choose a Physics-controlled mesh and Element size **normal**. Make sure that all 5 Contributors are used. **Build all**.

In **Study**, add **Parametric Sweep**. Add parameter **E** (Electric Field strength) and let it range from 5 to 25 in steps of 5: range(5,5,25). Add parameter **Q12** and let it range from -5 to -3 in steps of 0.1: range(-5,0.1,-3). Set Sweep type to **All combinations**. **Compute**.

In **Results**, under **Derived Values**, add **Volume Maximum** and select the Active Layer block. For Expression fill in **solid.disp**. Under **Displacement (solid)**, check or add **Surface**, under

Surface add **Deformation**, and add **Max/Min Volume**. Set expression to **solid.disp**. You will find your **displacement results visualized** in Displacement (solid). Here it is possible to change parameter values within the range set in the Parametric Sweep. For a **total overview of the displacement** values for all different parameter values, go to the Derived Values tab, to Volume Maximum. For the Parameter selection (E) & (Q12) select **All** and for Table columns set **Data only**. **Evaluate** to find all displacement magnitudes for every combination of parameters E and Q12.

3. Shell Module Film Model Guide

Introduction

In this file the process to create a model for an electrostrictive film using an adapted shell model in COMSOL is recorded. In this test setup, a film consisting of 1 electroactive layer and 1 passive layer is created, on the back side kept fixed to an 'immovable object'. On the top and bottom side the electroactive layer is sputtered with gold to create 2 opposing electrodes allowing for an electric field to be created.

COMSOL Model

In **Model Wizard**, select **3D**, then under **Structural Mechanics** select and add **Shell (shell)**. In **Study** select **Stationary**.

In **Global Definitions**, set the parameters as shown in Table 4.

Name	Expression	Value	Description
E	0.095 [GPa]	9.5E7 Pa	Young's Modulus electroactive material
v	0.22	0.22	Poisson's ratio electroactive material
k	1	1	Ratio between transverse strains and longitudinal strain induced purely by external electric field
M33	2E-18 [m ² /V ²]	2E-18 [m ² /V ²]	Electromechanical coupling coefficient longitudinal strain
M13	-k*M33	2E-18 [m ² /V ²]	Electromechanical coupling coefficient transverse (XZ-plane) strain
M23	-k*M33	2E-18 [m ² /V ²]	Electromechanical coupling coefficient transverse (YZ-plane) strain
E3	20 [MV/m]	2E7 V/m	Electric Field strength
lambda	$(E*v)/((1+v)*(1-2*v))$	3.0591E7 Pa	Lamé constant lambda
mu	$E/(2*(1-v))$	6.0897E7 Pa	Lamé constant mu
rho	1500 [kg/m ³]	1500 kg/m ³	Density of the electroactive material
d	0.150 [mm]	1.5E-4 m	Distance between the 2 electrodes (Thickness of the electroactive material)
dk	0.057 [mm]	5.7E-5 m	Thickness of the passive material
Width	11 [mm]	0.011 m	Width of the electroactive and passive

			material
--	--	--	----------

Table 4. Model parameters set in Parameters 1.

In **Geometry**, set **unit length** to **mm**. Create **2 blocks** as shown in table 5. Form a **Union**.

Block #	Block 1	Block 2
Name	'Passive Layer'	'Active Layer'
Width	Width/2	Width/2
Depth	45	45
Height	dk	d
[x,y,z] corner position	[0,0,d]	[0,0,0]

Table 5. Dimensions and position of the blocks.

In **Materials**, select **add Material from Library**, add **Kapton H (Polyimide tape) [solid]**. In Geometric Entity Selection, select all the 5 outside boundaries of the Passive Layer block. Assign it the following material properties shown in table 6.

Material property	Value
Young's Modulus (E)	8.46e+8 [Pa]
Poisson's ratio (nu)	0.34
Density (rho)	1.42[g/cm ³]

Table 6. Material properties Kapton H (polyimide tape).

In **Shell**, check if every block in the geometry is selected. Under Elastic Material 1, **change the name** of Linear Elastic Material 1 to **Linear Elastic Active Material**. Set the Solid Model to **Isotropic** and specify Young's **modulus** and **Poisson's ratio**. Set the 3 parameters to **User defined**. Define E as parameter **E**, v as parameter **v** and rho as parameter **rho**.

In the **Model Builder** select **Show more Options...** Enable **Equation View** by checkmarking the box and pressing OK. Open the Linear Elastic Active Material tab and go to **Equation View**. Find **Membrane part of second Piola-Kirchhoff stress (local), 11 component**, **Membrane part of second Piola-Kirchhoff stress (local), 22 component** and **Membrane part of second Piola-Kirchhoff stress (local), 33 component** (setting the description to alphabetical order makes this easier). **Alter their expressions** as shown in table 7.

Name	Standard Expression	Addition to the expression	Description
Shell.Sml11	shell.Sml11+shell.D11*shell.eeml11+2*shell.D14*shell.eeml12+shell.D12*shell.eeml22+shell.D13*shell.eeml33	-((lambda+2*mu)*M13+lambda*(M23+M33))*E3^2	Membrane part of second Piola- Kirchhoff

			stress (local), 11 component
Shell.Sml22	shell.Smil22+shell.D12*shell.eeml11+2*shell.D24*shell.eeml12+shell.D22*shell.eeml22+shell.D23*shell.eeml33	$-\left(\left(\lambda+2\mu\right)M_{23}+\lambda m_{\text{bda}}\left(M_{13}+M_{33}\right)\right)E_3^2$	Membrane part of second Piola- Kirchhoff stress (local), 22 component
Shell.Sml33	shell.Smil33+shell.D13*shell.eeml11+2*shell.D34*shell.eeml12+shell.D23*shell.eeml22+shell.D33*shell.eeml33	$-\left(\left(\lambda+2\mu\right)M_{33}+\lambda m_{\text{bda}}\left(M_{13}+M_{23}\right)\right)E_3^2$	Membrane part of second Piola- Kirchhoff stress (local), 33 component

Table 7. Altering of the second Piola-Kirchhoff stress expressions

Under Material Models, add **Linear Elastic Material**. Change the name of Linear Elastic Material 2 to **Linear Elastic Passive Material**. Select all **outside boundaries** of the Passive Layer block. This causes these boundaries to be overridden in Linear Elastic Active Material. Set the Solid model to **Isotropic** and specify Young's **modulus and Poisson's ratio**. Set the 3 parameters to **From material**.

Under Thickness and Offset 1, **change the name** of Thickness and Offset 1 to **Thickness and Offset Active Material**. Set the Thickness to **0.01 [mm]** and define the offset as **No offset**.

Add **Thickness and Offset**. Change the name of Thickness and Offset 2 to **Thickness and Offset Passive Material**. Set the Thickness to **(d+dk)/2** and define the offset as **No offset**.

Under Face Constraints, add **Fixed Constraint**. Select the back faces of both the Active Layer and Passive Layer block (at y=0).

Under Face Constraints, add **Symmetry**. Select the side faces of both the Active Layer and Passive layer block (at x=0).

In **Mesh**, set Mesh settings to User-controlled mesh. Under **Size** set Element Size to calibrate for **Semiconductor** and Predefined to **Normal**. Enable **Free Tetrahedral** and add **Corner Refinement**. Set Geometric entity level to Entire geometry. **Build all**.

In **Study**, add **Parametric Sweep**, Add parameter **E** (Electric Field strength) and let it range from 5 to 25 in steps of 5: range(5, 5, 25). Add parameter **M33** and let it range from 1E-18 to 3E-17 in steps of 0.1E-18: range(1E-18, 0.1E-18, 3E-17). Add parameter **k** and let it range from 0.5 to 1.0 in steps of 0.1: range (0.5, 0.1, 1.0) Set Sweep type to **All combinations**. **Compute**.

In **Results**, under **Derived Values**, add **Surface Maximum** and select all boundaries. For Expression fill in **shell.disp**. Add a new **3D plot group**, name it **Displacement (shell)**. Under Displacement (shell), add **Surface**, set the expression to **shell.disp**. Under Surface add **Deformation**. Add **Max/Min Surface**. Set expression to **solid.disp**. You will find your **displacement results visualized** in Displacement (shell). Here it is possible to change

parameter values within the range set in the Parametric Sweep. For a **total overview of the displacement** values for all different parameter values, go to the Derived Values tab, to Surface Maximum 1. For the Parameter selection (E) & (M33) select **All**, for (k) select **From list** and select a value. For Table columns set **Data only. Evaluate** to find all displacement magnitudes for every combination of parameters E and Q12 for a specific k value. (When all k values are evaluated at the same time, the table will become unorganized)

4. Shell Module Aligned Nanofiber Model Guide

Introduction

In this file the process to create a model for an electrostrictive nanofiber integrated mat using an adapted shell model in COMSOL is recorded. In this test setup, a film consisting of 1 layer of electroactive nanofiber integrated PDMS, 1 passive layer and 2 Carbon Black electrodes inside a PDMS layer is created, based on the model for an electrostrictive film using an adapted shell model in COMSOL. This instruction continues on the premade electrostrictive film using an adapted shell model.

COMSOL model

Load in the **electrostrictive film using an adapted shell model** file.

In **Global Definitions**, add a new **Parameters** tab. Name it **Orthotropic Material Property Parameters** and insert the parameters shown in table 8.

Name	Expression	Value	Description
Eft	4 [MPa]	5.3E7 Pa	Young's Modulus Fiber transverse direction
Efa	4 [MPa]	4E6 Pa	Young's Modulus Fiber axial direction
Em	0.795879 [MPa]	7.9588E5 Pa	Young's Modulus PDMS Matrix
Eplane	$E_{ft} \cdot V_f + E_m \cdot v_m$	2.2345E6 Pa	Young's Modulus mat X direction
Eaxial	$E_{fa} \cdot V_f + E_m \cdot v_m$	2.4236E7 Pa	Young's Modulus mat Y direction
v _{xy}	0.27	0.27	Poisson ratio fiber XY
v _{yz}	0.01	0.01	Poisson ratio fiber YZ
M _m	0.49	0.49	Poisson ratio PDMS matrix
v _h	$v_{xy} \cdot V_f + M_m \cdot V_m$	0.43699	Poisson ratio mat longitudinal to transverse
v _p	$v_{yz} \cdot V_f + M_m \cdot V_m$	0.85369	Poisson ratio mat transverse
G _{f12}	0.5 [GPa]	5E8 Pa	Shear Modulus Fiber 12 plane
G _{f23}	$E_{plane} / (2 \cdot (1 + v_p))$	8.7664E5 Pa	Shear Modulus Fiber 23 plane
G _{f13}	0.5 [GPa]	5E8 Pa	Shear Modulus Fiber 13 plane
G _m	250 [kPa]	2.5E5 Pa	Shear Modulus PDMS matrix
V _f	0.449	0.449	Fraction composite fibers

Vm	0.551	0.551	Fraction composite matrix
rhof	4.612E-4 [g/mm ³]	461.2 kg/m ³	Density fiber
rhom	965 [kg/m ³]	965 [kg/m ³]	Density matrix

Table 8. Orthotropic Material Property Parameters.

This leaves the other list of parameters **parameters** looking like as shown in table 9.

Name	Expression	Value	Description
k	0.7	0.7	Ratio between transverse strains and longitudinal strain induced purely by external electric field
M33	5E-18 [m ² /V ²]	5E-18 [m ² /V ²]	Electromechanical coupling coefficient longitudinal strain
M13	-k*M33	2E-18 [m ² /V ²]	Electromechanical coupling coefficient transverse (XZ-plane) strain
M23	-k*M33	2E-18 [m ² /V ²]	Electromechanical coupling coefficient transverse (YZ-plane) strain
E3	20 [MV/m]	2E7 V/m	Electric Field Strength
d	0.100 [mm]	1E-4 m	Distance between the 2 electrodes (Thickness of the electroactive material)
dk	0.057 [mm]	5.7E-5 m	Thickness of the passive layer
de	0.100 [mm]	1E-4 m	Thickness of the electrodes
Width	11 [mm]	0.011 m	Width of the electroactive and passive layer

Table 9. Parameters left in parameters 1.

In **Geometry**, for each element, change the **Width** to **50 mm** and the Depth to **Width/2**. Furthermore, create 2 new blocks with dimensions as shown in table 10.

Block #	Block 1	Block 2
Name	'Upper Electrode'	'Lower Electrode'
Width	50	50
Depth	Width/2	Width/2
Height	de	de

[x,y,z] corner position	[0,0,d+de]	[0,0,0]
-------------------------	------------	---------

Table 10. Dimensions of the new blocks.

Furthermore, increase the corner position in z for the P(VDF-TrFE-CTFE) block with '+de' and increase the corner position of the Kapton Tape with '+2*de'.

In **Materials**, search for PDMS - Polydimethylsiloxane and assign it to the 2 new 'electrode' blocks.

In **Shell**, under Linear Elastic Active Material, change the Solid model from Isotropic to **Orthotropic**. Set Material data ordering to **Standard (11, 22, 33, 12, 23, 13)**. Set the Young's Modulus, Poisson's ratio, Shear Modulus and Density all to **User defined**. Fill in the lines as follows:

Young's Modulus:

- Eaxial
- Eplane
- Eplane

Poisson's ratio:

- vh
- vp
- vh

Shear Modulus:

- $(Gf12*Gm)/(Vm*Gf12+Gm*Vf)$
- $Eplane/(2*(1+vp))$
- $(Gf13*Gm)/(Vm*Gf13+Gm*Vf)$

Density:

- $\rho_{of}*Vf+\rho_{om}*Vm$

In **Shell**, add a new **Linear Elastic Material** model, name it 'Linear Elastic Electrode Material'. Select the 2 'Electrode' blocks. Also add 'Thickness and Offset', name it 'Thickness and Offset Electrode Material'. Insert $(de*2+d)/3$. In 'Thickness and Offset Passive Material' change the the thickness to $(d+dk+de*2)/4$.

Open the Linear Elastic Active Material tab and go to **Equation View**. Find **Membrane part of second Piola-Kirchhoff stress (local), 11 component**, **Membrane part of second Piola-Kirchhoff stress (local), 22 component** and **Membrane part of second Piola-Kirchhoff stress (local), 33 component** (setting the description to alphabetical order makes this easier). **Alter their expressions** as shown in table 10.

Name	Standard Expression	Addition to the expression	Description
------	---------------------	----------------------------	-------------

Shell.Sml11	shell.Smil11+shell.D11*shell.eeml11+2*shell.D14*shell.eeml12+shell.D12*shell.eeml22+shell.D13*shell.eeml33	$-(2*((vp*Eplane)/(lambda-lambda*vh-2*vp^2))*M13+(1-vh*Eplane)/(lambda-lambda*vh-2*vp^2))*M33)*E3^2$	Membrane part of second Piola- Kirchhoff stress (local), 11 component
Shell.Sml22	shell.Smil22+shell.D12*shell.eeml11+2*shell.D24*shell.eeml12+shell.D22*shell.eeml22+shell.D23*shell.eeml33	$-(((Eplane*(lambda*vh+vp^2))/((lambda-lambda*vh-2*vp^2)*(1+vh)))*M13+((Eplane*(lambda-vp^2))/((lambda-lambda*vh-2*vp^2)*(1+vh)))*M23+((vp*Eplane)/(lambda-lambda*vh-2*vp^2))*M33)*E3^2$	Membrane part of second Piola- Kirchhoff stress (local), 22 component
Shell.Sml33	shell.Smil33+shell.D13*shell.eeml11+2*shell.D34*shell.eeml12+shell.D23*shell.eeml22+shell.D33*shell.eeml33	$-(((Eplane*(lambda*vh+vp^2))/((lambda-lambda*vh-2*vp^2)*(1+vh)))*M13+((Eplane*(lambda-vp^2))/((lambda-lambda*vh-2*vp^2)*(1+vh)))*M23+((vp*Eplane)/(lambda-lambda*vh-2*vp^2))*M33)*E3^2$	Membrane part of second Piola- Kirchhoff stress (local), 33 component

Table 10. Altering of the second Piola-Kirchhoff stress expressions for orthotropic nanofiber model.

In **Mesh** select **Build All**.

In **Study**, perform a **Parametric Sweep** for E3 for 5, 10, 15, 17.5, 20 and 22.5 MV/m, for parameter **M33** ranging from 3E-18 to 8E-18 in steps of 1E-18: range(3E-18, 1E-18, 8E-18), and for parameter **k** ranging from 0.5 to 1.0 in steps of 0.1: range (0.5, 0.1, 1.0) Set Sweep type to **All combinations**. **Compute**.

Find the results in the same way as found in the file **electrostrictive film using an adapted shell model**.

5. Shell Module Transversely Aligned Nanofiber Model Guide

Introduction

In this study it was also attempted to create a model modelling the electromechanical response of a transverse aligned nanofiber integrated PDMS mat. Unfortunately, this attempt had to be aborted. Although a definitive model was created for modelling the transverse aligned nanofiber integrated PDMS mat, the process to create the insufficient model is included in this appendix for someone to continue on. In this test setup, a film consisting of 1 layer of electroactive nanofiber integrated PDMS, 1 passive layer and 2 Carbon Black electrodes both inside a PDMS layer is created, based on the model for an aligned P(VDF-TrFE-CTFE) nanofiber integrated PDMS mat using an adapted shell model in COMSOL. This instruction continues on the premade electrostrictive nanofiber integrated PDMS mat using an adapted shell module.

Load in the **P(VDF-TrFE-CTFE) nanofiber integrated PDMS mat** file.

In **Geometry**, change the orientation of all blocks by replacing the Width with the Depth and vice versa, as shown in table 11.

Name block	Old Size and Shape	New Size and Shape
Kapton Tape	Width: 50 [mm] Depth: Width/2	Width: Width/2 Depth: 50 [mm]
Upper Electrode	Width: 50 [mm] Depth: Width/2	Width: Width/2 Depth: 50 [mm]
P(VDF-TrFE-CTFE)	Width: 50 [mm] Depth: Width/2	Width: Width/2 Depth: 50 [mm]
Lower Electrode	Width: 50 [mm] Depth: Width/2	Width: Width/2 Depth: 50 [mm]

Table 11. New configuration of the Size and Shape of the model

Reasoning behind the change in orientation of all blocks for the transverse aligned nanofibers
 The nanofibers can be laid transversely aligned instead of aligned in the P(VDF-TrFE-CTFE) block using 2 methods: 1. Rotating the nanofibers, or 2. Rotating everything but the fibers. 1. By rotating the fibers from pointing in the X-direction to pointing in the Y-direction, they would be transversely aligned in the PDMS mat. This would be done by exchanging the altered constitutive equations for the xx-direction and yy-direction Piola-Kirchhoff stresses. But when this method is used, this would cause the model to be further changed in the linear elastic material part, since the axes of the model and the axes of the Poisson's ratios would not connect perfectly to each other. Therefore method 2. would be an easier method for transversely aligning the nanofibers. By changing everything but the direction of the nanofibers, the axes stay the same for the nanofibers. Only the fixed constraints and symmetry constraints will have to be changed. The constitutive equations also stay the same, since the axis of symmetry and symmetry plane remain the same. The problem with the model encountered after

this change is the switch of direction of bending of the electroactive material. This should be in the direction of the passive material, but this is the other way around.

6. Excel data sheets:

The excel data sheets can be formally asked for via email contact